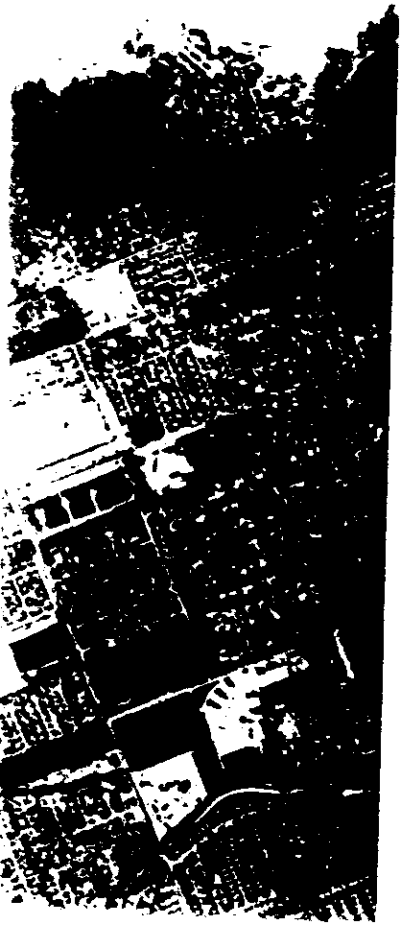

[redacted]

Copy No. [redacted]

PERFORMANCE ANALYSIS FOR THE 1101 SYSTEM

1 FEBRUARY 1968

CONTRIBUTORS: [redacted]

Itek OPTICAL SYSTEMS DIVISION

ITEK CORPORATION • 10 MAGUIRE ROAD • LEXINGTON, MASSACHUSETTS 02173

[redacted]

CONTENTS

FIGURES

TABLES

1. SUMMARY

In general, the performance of the 1101 system was good and it operated both mechanically and electrically as well as expected. However, photographically, the 1101 system did not completely meet our expectations. In fact, both panoramic cameras did not reach their peak performance levels during the mission because they operated slightly out of focus. Despite this anomaly, which is further explained in the Introduction (Section 2), "the best photography of mission 1101 is equal to or better than any previous KH-4 photography. The best photography from 1101 was obtained with the forward-looking camera. The aft-looking camera produced softer imagery than normally obtained with the KH-4 system . . ." "Several CORN and fixed resolution targets were recorded . . ." "The best targets observed yielded approximately a 6-foot ground resolved distance along the line of flight (IMC direction), and 10 feet across the line of flight (scan direction)." "The image quality of the forward camera photography recovered from mission 1101-2 is judged to be good and comparable to the best ever produced by the KH-4 camera system."

The above quotations were taken from the PET report for mission 1101.

It is also worth mentioning that the 1101 mission photography was given an MIP rating of 95. The MIP rating is assigned by NPIC and is intended to be indicative of the mission information potential for the best photography acquired. The highest MIP rating ever given to a KH-4 was 90. The performance of the 1101 system reveals an engineering and technological achievement, since the KH-4B system is considerably more complex than the KH-4 system and 1101 was the first KH-4B system flown.

The performance of the 1101 system has been analyzed and the following conclusions have been reached:

1. The forward-looking and aft-looking panoramic cameras were out of focus by 0.001 and 0.002 inch, respectively, because the air-to-vacuum focus shift of the optics was 0.014 inch instead of 0.016 inch as anticipated.

2. Resolution predictions have been computed for the CORN and HPL targets using laboratory and mission data. A favorable correlation has been demonstrated between the CORN target actual readings and the predictions.

3. The relationship between dynamic resolution and image smear should be determined experimentally for each panoramic camera. In addition, we have found that the relationship between dynamic resolution and image smear can be described by Equation (3.13).

4. By utilizing accurate laboratory and mission data, it is possible to predict the camera resolution almost as accurately as it is to determine it in the laboratory.

5. Edge trace analysis has produced resolution predictions which do not correlate with the actual CORN target readings.

6. In the A takeup experiment, three separate properties of the 3404 film were investigated.

a. Threshold resolution curve
b. RMS granularity
c. Modulation transfer function.

It appears that these properties of the film are not altered appreciably by the mission environment.

7. The density analysis of the HPL targets showed that most of the targets were properly exposed.

2. INTRODUCTION

In the summary it was indicated that both panoramic cameras operated slightly out of focus. How this unfortunate incident occurred can be best understood by describing the procedure used in determining and adjusting the operational focal plane.

Operationally, the peak focus position (essentially the distance along the lens optical axis from a well defined surface on the lens cell, at which the three-bar resolution of the lens is maximum) depends solely on the optics (Petzval lens). The actual distance of the film from the lens during exposure depends on film dynamics and the mechanical distance of the focal plane rollers from the lens. The purpose of the focusing procedure is to determine the operational peak focus position. When this dimension is established, the focal plane rollers are adjusted to the lens cell so that the film will be dynamically positioned at the focal plane of maximum resolution. When the camera is operating, the film is lifted about 0.001 inch above the focal plane rollers during exposure. The peak focus position is determined by utilizing a collimator and a three-bar target is placed at the infinity focus of the collimator (collimator infinity focus is previously determined by an autocollimation technique). The image of the three-bar target emerging from the Petzval lens is examined visually with the aid of a microscope. The microscope is translated longitudinally along the optical axis until maximum resolution is observed. At this position the microscope is focused on the three-bar image located at the peak focus position of the lens. Then, the distance that the microscope must be translated in order to focus it on the back surface of the field flattener (an integral part of the Petzval lens) is equal to the distance that separates the field flattener from the peak focus position. This distance is called the back focal length of the lens and it is utilized in the adjustment of the focal plane rollers with respect to the field flattener. This test is conducted under ambient conditions (normal temperature and pressure). Unfortunately, Petzval lenses display a shift in peak focus when operating in a vacuum. This is quite normal for all refractive optics but it is very essential that this shift be determined accurately for the Petzval lenses since the KH-4B systems operate in vacuum during the flight. Prior to the 1101 flight, all known theoretical evidence indicated that the air-to-vacuum focus shift of the Petzval lenses was 0.016 inch towards the field flattener and the 1101 was focused in the laboratory accordingly. However, when the 1101 photography was visually examined after the mission, it was obvious that the cameras had operated slightly out of focus. In addition, it was determined that the vacuum peak focus was slightly beyond the operational film position. In other words, the film was between the lens and the vacuum peak focus position when it was exposed. It appears that the air-to-vacuum focus shift was not as large as was expected. Since the 1101 flight, some very elaborate tests have been run at our West Coast facility. These tests and their results are described in a separate report,* but essentially the findings are that the air-to-vacuum focus shift was actually about 0.014 to 0.0145 inch. In addition, a new theoretical computation of the air-to-vacuum focus shift based on a more accurate formula recently published by NBS showed that the

*Preliminary Tests Results [redacted]

air-to-vacuum focus shift should be 0.014 inch. Furthermore, our detailed analysis (described in this report) of CORN target resolutions achieved by the 1101 and other laboratory data indicates that in the aft camera (unit no. 302) the peak focus was about 0.002 inch beyond the film plane while in the forward camera (unit no. 303) the peak focus was about 0.001 inch beyond the film plane. These observations of the actual focus conditions of both instruments are compatible with an air-to-vacuum focus shift of 0.014 inch.

The purpose of this report is to describe the most important results of the analysis that has been conducted following the flight of the 1101 system. The analysis attempted to determine the performance level of the 1101 system and to explain the factors which affected this performance level. The performance criterion which we have utilized is the familiar three-bar resolution. From preflight laboratory data and the mission ephemeris, we have predicted the three-bar resolution levels of the system. An independent assessment of these levels is derived from CORN targets that were deployed at various locations and were covered by the 1101 photography during engineering passes. The system performance is discussed more thoroughly in Section 3 of this report and it is shown that there is good correlation between the resolution levels indicated by the CORN targets and those predicted from ephemeris and laboratory data. However, the resolution predictions derived from edge target analysis do not correlate with the CORN target resolutions.

Section 4 discusses the results of the A takeup experiment which was an investigation of the properties of the 3404 film. Section 5 describes the density analysis of the HPL targets and the conclusions as to the proper exposure of these targets.

In Appendix B of this report, we have listed our resolution predictions for a number of HPL targets that were covered by the 1101 photography. These resolution predictions should be of particular interest to the photointerpreters. However, we must emphasize that one should be very careful in using these resolution predictions. There is no direct relationship between three-bar ground resolution and dimensions of objects. In fact, there are a lot of real objects with dimensions considerably smaller than the three-bar resolution which have been successfully interpreted. Therefore, we recommend that the predicted three-bar resolution values for HPL targets should be empirically correlated to the objects recognized by the photointerpreters. This could be achieved by collecting precise ground detail data at the locations of domestic targets of interest.

3. SYSTEM PERFORMANCE

3.1 CORN TARGET RESOLUTION

Each CORN target deployed consisted of the 51/51 T-bar target, a Gray scale target, and a 100-foot edge target. These targets are described in Figs. 3-1, 3-2, and 3-3.

As shown in Fig. 3-1, the 51/51 T-bar consists of two perpendicular arrays of three-bar targets. From panels 3 to 9, the size of the three-bar targets decreases in steps of the sixth root of two ($\sqrt[6]{2}$). In panel 1, the width of a white bar is 8 feet, corresponding to a ground resolution of 16 feet per cycle. Panels 2 and 3 contain three-bar targets with spatial periods of 12 and 8 feet per cycle, respectively. Since 1101 operated in a defocused condition, only panels 1, 2, and 3 were actually utilized in determining resolution. Thus, the resolution readings obtained (from the original negatives) are very coarse. If a $\sqrt[6]{2}$ progression existed between panels 1 and 3, there would have been five panels between 1 and 3 rather than just one panel (panel 2). In addition, on some frames the 16-foot target (panel 1) was not resolved, pointing to the need of three-bar targets larger than that of panel 1. In conclusion, the CORN target display proved to have an insufficient number of frequencies for the 1101 system analysis.

The T-bar targets were laid on the ground with one of the arrays approximately parallel to the vehicle ground track and the other approximately perpendicular to it. Therefore, on the panoramic format, one of the arrays gives the resolution in the along-track direction (short dimension of the format) and the other in the cross-track direction (long dimension of the format).

The CORN target images which are present in the original negatives of both panoramic cameras were examined by three NPIC photointerpreters and our own photointerpreter. The NPIC observers consistently read higher than our own photointerpreter. This is not unusual since a recent survey showed that there are many definitions of resolution due to the variance in interpretation between resolution readers. Most resolution readers, with the aid of microscopes, see the same thing when examining a resolution target. However, they may differ significantly when interpreting the target or essentially deciding which of the three-bar targets determines the resolution level. This decision process is controlled by a conscious or subconscious interpretation of definition of resolution. There is no reason to believe that one interpretation of resolution is any better than other interpretations. However, a lot of preflight resolution data is generated on every KH-4B system and it becomes necessary, for comparison purposes, to utilize CORN target readings that have been obtained under rules similar to those used in determining camera resolution in the laboratory. Therefore, we believe that the CORN targets on the original negative should be read by the same individuals who evaluate resolution targets in the laboratory. We know the laboratory resolution readings are relatively conservative. Therefore, for every CORN target image in the original negatives, we have used the most conservative reading available. The results are shown in Tables 3-1 and 3-2 for the forward- and aft-looking cameras, respectively, under the columns identified as Ground Resolution, feet.

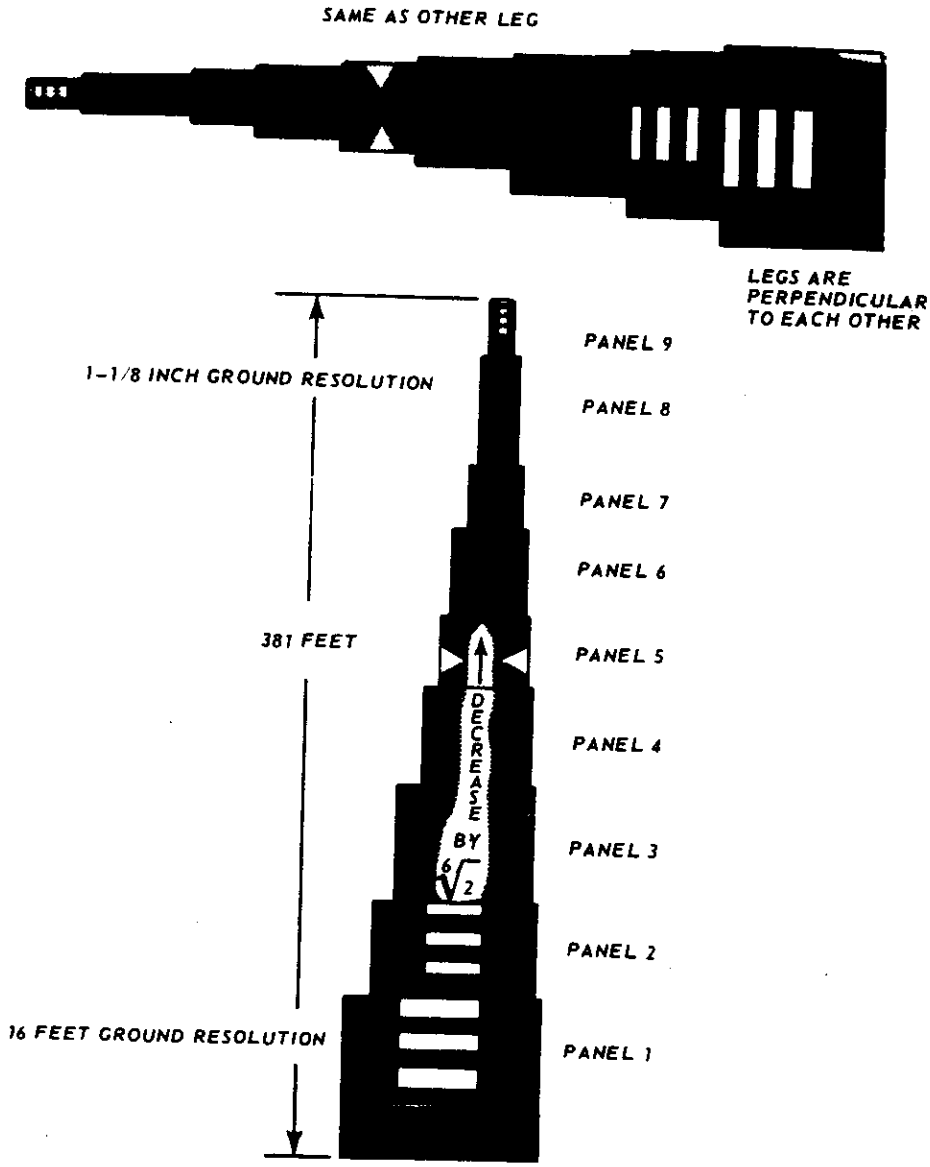

Fig. 3-1 — The 51/51 T-bar target

The Gray Scale Target consists of five (5) panels varying from 4% reflectance to 64% reflectance. The reflectance values are as follows:

Panel No. 1. 4%
2. 8%
3. 16%
4. 32%
5. 64%

Each panel is 20 x 20 feet. The target is laid out perpendicular to the line of flight and is 20 x 100 feet.

Instrumentation and operation will be carried out according to normal CORN operations.

Fig. 3-2 — The Gray scale target

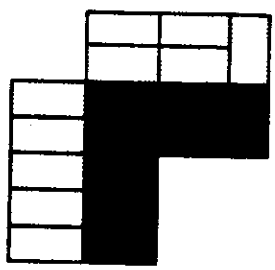

Fig. 3-3 — The 100-foot edge target

Table 3-1 — CORN Target Resolution of Forward Camera

Pass	Frame	Along Track			Cross Track		
		Ground Resolution, feet	System Resolution, l/mm	Apparent Target Modulation	Ground Resolution, feet	System Resolution, l/mm	Apparent Target Modulation
14	13	16	76	0.427	>16	<80	0.403
14	31	8-12	88-132	–	8-12	87-130	0.422
16	5	>16	<78	0.145	>16	<91	0.170
63	5	10 FX	–	–	>16 FX	–	–
111	22	12-16 DP	60-80	–	>16 DP	<59	0.190
127	13	8.58 FX / NPIC	121	–	>16 FX / NPIC	<71	–
127	15	10.8 FX / DP	88	–	>16 FX / DP	<58	–
127	23	8-12	75-112	0.278	12-16	55-73	0.315
143	20	8-12	76-113	0.357	12-16	55-73	0.344
157	9	7.12-8	116-131	0.427	8-12	74-112	0.408
173	19	8-12	74-111	0.457	12	73	0.446

Definitions: FX = Fixed target
DP = Reading available on duplicate positive only
NPIC = Reading by NPIC only

Table 3-2 — CORN Target Resolution of Aft Camera

Pass	Frame	Along Track			Cross Track		
		Ground Resolution, feet	System Resolution, l/mm	Apparent Target Modulation	Ground Resolution, feet	System Resolution, l/mm	Apparent Target Modulation
14	19	>16	<76	0.422	>16	<80	0.385
14	37	>16	<67	–	12-16	65-87	0.315
16	11	12	102	0.301	>16	<91	0.245
111	28	>16 DP	<58	–	>16 DP	<58	0.329
127	19	13.8 FX / DP	67	–	>16 FX / DP	<57	–
127	29	>16	<57	0.315	>16	<55	0.329
143	26	>16	<57	0.365	>16	<55	0.375
157	16	>16	<58	0.457	16	56	0.422
173	25	>16	<57	0.417	>16	<55	0.474

Definitions: FX = Fixed target
DP = Reading available on duplicate positive only

On Tables 3-1 and 3-2, the first two numbers in the columns labeled Pass and Frame uniquely identify the frame on which the image of a specific CORN target display appears. (The actual geographic locations of the CORN target displays are shown in Table 3-3.) The two major columns labeled Along Track and Cross Track indicate that the resolution information pertains to the directions of the y coordinate and x coordinate, respectively, as these orthogonal coordinates have been defined by NPIC. The columns labeled Ground Resolution are the actual readings. Whenever the 16-foot target was not resolved, the entry is >16, meaning larger than 16 feet. The entry 12-16 indicates that the 16-foot target was resolved but the 12-foot one was not. Since there were no targets between 12 and 16 feet, we must assume that the actual resolution was somewhere between 12 and 16 feet. The entry 12 indicates that the 12-foot target was resolved but its image was poor so we assumed that the actual resolution was 12 feet. The letters FX following a number indicate that the target was actually a fixed target and not a deployed CORN target. Most fixed targets are quite differently arranged than the T-bar target described in Fig. 3-1. The letters DP indicate that the resolution reading was obtained from a duplicate positive. The resolution reading of the same target on the original negative was not available. The letters NPIC indicate that the number came from the NPIC group but could not be compared to any other readings as none were available and, therefore, there is no way of knowing whether it is a conservative or optimistic reading. The columns labeled System Resolution contain numbers, in lines per millimeter, derived from the adjacent ground resolution numbers through a scale factor that is affected by vehicle altitude as well as by the location of the target image on the panoramic format. In this column, the entry <80 means that the film resolution was less than 80 lines per millimeter and the entry 60-80 means that the film resolution was between 60 and 80 lines per millimeter.

The columns labeled Apparent Target Modulation indicate the modulation of the T-bar target as seen through the atmosphere. The modulation, m, of a three-bar target is defined by:

$$m = \frac{I_{max} - I_{min}}{I_{max} + I_{min}} \qquad (3.1)$$

where I_{max} = brightness of a bar
I_{min} = brightness of background

Contrast, C, is defined by:

$$C = \frac{I_{max}}{I_{min}} \qquad (3.2)$$

Modulation and contrast are related by the formula:

$$m = \frac{C - 1}{C + 1} \qquad (3.3)$$

Therefore, the modulation of the T-bar target on the ground, M_{TG}, is:

$$M_{TG} = \frac{IR_{max} - IR_{min}}{IR_{max} + IR_{min}} = \frac{R_{max} - R_{min}}{R_{max} + R_{min}} \qquad (3.4)$$

Table 3-3 — CORN Target Coverage

Pass	Frame	x	y	Location
14	13 fwd	64.3	1.6	Buffalo, New York
	19 aft	10.9	0.5	42°56'N, 78°55'W
14	31 fwd	48.1	4.4	Johnstown, Pennsylvania
	37 aft	27.4	2.3	40°20'N, 78°55'W
16	5 fwd	73.8	2.3	Navato, California
	11 aft	1.3	4.4	38°8'N, 122°33'30"W
63	5 fwd	–	–	Holloman AFB
	11 aft	–	–	Alamogordo, New Mexico, Fixed Target 33°6'N, 106°20'W
111	22 fwd	23.8	1.2	–
	28 aft	52.0	5.1	–
127	13 fwd	68.2	3.5	Indian Springs, Nevada, Fixed Target 36°42'N, 115°29'W
	19 aft	7.1	2.8	
127	15 fwd	50.2	1.3	Fixed Target
	21 aft	24.5	5.2	
127	23 fwd	41.8	4.1	Baker, California
	29 aft	33.6	2.5	35°14'N, 116°05'W
143	20 fwd	42.0	2.6	Tehacapi, California
	26 aft	32.2	3.8	35°7'N, 118°26'W
143	23 fwd	61.6	2.7	Edwards AFB, California
	29 aft	13.6	3.5	Fixed Target
157	9 fwd	32.2	1.2	Williamsport, Pennsylvania
	16 aft	43.2	1.0	41°15'N, 76°55'W
173	19 fwd	40.8	4.0	DuBois, Pennsylvania
	25 aft	34.6	2.9	41°13'N, 78°53'W

where I = solar illumination
R_{max} = reflectance of the white bars
R_{min} = reflectance of the black background

From the CORN target manual:

$$R_{max} = 33 \text{ percent}$$

$$R_{min} = 7 \text{ percent} \tag{3.5}$$

Hence,

$$M_{TG} = 0.65 \tag{3.6}$$

However, the modulation of the T-bar target, as seen from the vehicle, is greatly reduced because of atmospheric attenuation and luminance. Thus, the apparent modulation of the target as seen from the vehicle, M, is:

$$M = \frac{(IR_{max}\,T + A) - (IR_{min}\,T + A)}{(IR_{max}\,T + A) + (IR_{min}\,T + A)} \tag{3.7}$$

where T = atmospheric transmission
A = atmospheric luminance

The modulation, M, in Equation (3.7) cannot be determined unless the unknowns A and T are replaced by known quantities. We observe, though, that A and T also affect the apparent contrast of the 100-foot edge target as follows:

$$C_{EA} = \frac{Ir_{max}\,T + A}{Ir_{min}\,T + A} \tag{3.8}$$

where r_{max} = maximum reflectance of edge target
r_{min} = minimum reflectance of edge target
C_{EA} = apparent contrast of edge target as seen from the vehicle

Equation (3.8) can be solved for A in terms of C_{EA} as follows:

$$A = \frac{IT(r_{max} - C_{EA}\,r_{min})}{C_{EA} - 1} \tag{3.9}$$

Equation (3.9) is now substituted into Equation (3.7). Thus,

$$M = \frac{IT(R_{max} - R_{min})}{IT(R_{max} + R_{min}) + 2IT\,\dfrac{(r_{max} - C_{EA}\,r_{min})}{C_{EA} - 1}}$$

$$= \frac{(C_{EA} - 1)(R_{max} - R_{min})}{(C_{EA} - 1)(R_{max} + R_{min}) + 2(r_{max} - C_{EA}\,r_{min})} \tag{3.10}$$

From the CORN target manual:

$$r_{max} = 37 \text{ percent}$$

$$r_{min} = 3 \text{ percent}$$

Therefore, the apparent T-bar target modulation as seen from the vehicle can be computed from the apparent edge target contrast, C_{EA}, and Equation (3.10). The term C_{EA}, in turn, is determined by tracing the edge target image with a microdensitometer. The maximum and minimum densities recorded by the microdensitometer, D_{max} and D_{min}, are utilized in conjunction with the D-log E curve of the film to determine log E_{max} and log E_{min}. The difference of these two values is the logarithm of C_{EA}. In other words,

$$\log E_{max} - \log E_{min} = \log \left(\frac{E_{max}}{E_{min}} \right) = \log C_{EA} \tag{3.11}$$

In conclusion, the modulations appearing in Tables 3-1 and 3-2 were obtained as follows:

1. AFSPPF traced the 100-foot edge target images on the original negatives.
2. D_{max} and D_{min} were obtained from each microdensitometer trace.
3. The respective log E_{max} and log E_{min} were determined using the D-log E curve.
4. The respective C_{EA} were computed utilizing Equation (3.11).
5. Finally, the modulations were obtained using Equation (3.10).

The significance of the apparent modulation of the T-bar target is the fact that the system resolution is affected by the target modulation.

Table 3-3 is self-explanatory. Columns x and y give the coordinates of the target images in the panoramic format. The coordinate system is that established by NPIC.

3.2 DETERMINATION OF OPERATIONAL RESOLUTION

3.2.1 Introduction

The three-bar ground resolved distance achieved by a panoramic camera at a specific geographic location depends entirely on the three-bar resolution of the image on the original negative at the corresponding point in the format. This is the so-called dynamic system resolution in line-pairs per millimeter or essentially the cycles per millimeter that appear on Tables 3-1 and 3-2. In turn, the dynamic system resolution depends on the static lens/film resolution and the image motion smear introduced during exposure by the dynamics of camera operation as well as other geometric and vehicle sources. When there is no relative motion between the image and the film motion, the dynamic system resolution is equal to the static resolution. Since various amounts of motion or smear always exist, the dynamic system resolution is consistently degraded below the static resolution level. In order to determine the operational or dynamic resolution, we establish the static lens/film resolution from laboratory data and compute the corresponding image motion smear from the ephemeris and SRV tape recorder data. The static lens/film resolution and the smear are then combined into a formula from which the dynamic resolution is computed. The formula that has been used very often is the following:

$$\frac{1}{R_d^2} = \frac{1}{R_s^2} + b^2 \tag{3.12}$$

where R_d = dynamic resolution
R_S = static resolution
b = image smear

It should be noted that there is no physical justification for this formula and that, at best, it comprises only a very rough approximation. We have found that it is necessary to determine the relationship between R_d, R_S, and b experimentally. In this manner, one obtains an experimental curve of R_d versus b. When b = 0, then $R_d = R_S$. An expression of the form

$$R_d = \frac{R_S}{[1 + (bR_S)^{E_1}]^{E_2}} \tag{3.13}$$

where E_1 and E_2 are experimentally determined exponents, is then fitted to the experimental curve. In other words, the exponents E_1 and E_2 are selected such that Equation (3.13) and the experimental curve give identical results. Equation (3.13) has no physical significance other than it is a mathematical function which describes the behavior of the experimental curve. Note that Equation (3.13) reduces to Equation (3.12) by setting $E_1 = 2$ and $E_2 = 1/2$. The shape of the resolution versus image smear curve and the value of R_S depends on the Petzval lens as well as the distance of the film from the peak focus position of the lens. It should be obvious from Equation (3.13) that the shape of the resolution versus image smear curve affects the exponents E_1 and E_2. We have found experimentally that if the film is displaced from the peak focus position, not only does R_S reduce, but E_1 and E_2 change values. Therefore, in order to compute the dynamic resolution, we utilize Equation (3.13) with exponents E_1 and E_2 determined from the corresponding resolution versus image smear experimental curve. This curve is obtained by performing laboratory dynamic resolution tests on the corresponding panoramic camera. During the resolution tests, the camera is focused at the anticipated operational peak focus position and known amounts of image smear are selectively introduced by mismatching the target wheel speed to the FMC rate of the camera. However, these dynamic resolution tests were not run on the 1101 system because of time schedule limitations. It is doubtful that they would have been very valuable anyway, because both cameras did not operate in flight at their peak focus positions.

In order to obtain some information about the exponents E_1 and E_2, several resolution versus image smear tests on unit no. 299 were run. One of the tests was run with the film at peak focus, another with the film 0.001 inch short of peak focus (simulating unit no. 303), and a third test with the film 0.002 inch short of peak focus (simulating unit no. 302). While individual Petzval lenses may display differences in their resolution performances at their peak focus positions, these differences are minimized when the lenses are all defocused by equal amounts. Therefore, we feel justified in using, in the 1101 analysis, the exponent values E_1 and E_2 obtained from the unit no. 299 resolution versus image smear tests. In fact, we have used the following values (obtained from the unit no. 299 resolution versus image smear tests) for E_1 and E_2 in our resolution predictions for the CORN targets and HPL targets:

1. For low contrast, $E_1 = 2.0$ and $E_2 = 0.65$.
2. For high contrast, $E_1 = 1.90$ and $E_2 = 0.63$.

3.2.2 Static Resolution

The determination of the static resolution, R_S, is very important for the 1101 analysis. This fact is accentuated by the out of focus conditions of both instruments because, while 1101's

performance was limited by the out of focus conditions of the Petzval lenses, it was only affected to a minor degree by image motion smear.

In order to determine R_S, we utilized the static resolution versus focus position tests that were performed on the respective Petzval lenses at our Lexington facility. These tests are performed by our optics group upon final assembly of the lens optical elements and before the lens is assembled on the panoramic camera. The tests are done on a Mann Optical Bench using a parabolic collimator, high contrast and low contrast (2:1) three-bar resolution targets, 3404 film, and the primary filter (Wratten no. 21). The angular field of the Petzval is essentially one-dimensional (in the y or along-track direction of the panoramic format). The total angular field of view is about 5 degrees (±2.5 degrees from the center).

During these static resolution tests, the focal position occupied by the 3404 film samples is varied in increments of 0.001 inch and the film/lens resolution is determined at seven positions across the lens angular field, i.e., 0, ±1, ±2, and ±3 degrees. Figs. 3-4 and 3-5 show the results of these tests, for units no. 302 and 303, at the center of the angular field (0 degrees). Similar curves have been plotted for the other field positions (±1, ±2, and ±3 degrees). Another problem with unit no. 303 is that the data of Fig. 3-5 were obtained with a Wratten no. 21 filter while the primary filter for unit no. 303 was a Wratten no. 23A. There is a slight decrease in resolution when the Wratten no. 23A filter is used instead of the Wratten no. 21.

Figs. 3-6 and 3-7 show the dynamic resolution versus focus curves for unit no. 303. The tests from which the curves were obtained were identical, except that a Wratten no. 21 filter was used in Fig. 3-6 and a Wratten no. 23A in Fig. 3-7. Also, the 0 focus positions in these figures are not the same. From the shape of the curves, it seems that the 0 focus position in Fig. 3-6 coincides with the -1 focus position in Fig. 3-7. So, if the curves in Fig. 3-7 were shifted to the right by 0.001 inch and compared to the corresponding curves of Fig. 3-6, one would find that, on the average, the curves of Fig. 3-7 have resolution values lower than the corresponding curves of Fig. 3-6 by approximately a factor of 1.2. Therefore, an approximate technique (with unit no. 303) for obtaining static resolution versus focus curves when using a Wratten no. 23A filter consists of taking the corresponding curves determined with a Wratten no. 21 filter and dividing them by 1.2. We have utilized this technique in obtaining approximate resolution versus focus curves for unit no. 303 (and a Wratten no. 23A filter) for all angular field positions except at the center of the field (0-degree angular field). At this field position, more accurate results can be obtained directly from Fig. 3-7.

The results of limited laboratory tests show that the operation of a panoramic camera in the laboratory produces about 2 microns of image smear. This amount of smear was combined with the dynamic resolution curves of Fig. 3-7 into Equation (3.13) (b = 2 microns, R_d from Fig. 3-7). Equation (3.13) was then solved for R_S. The result is the static resolution versus focus curves plotted in Fig. 3-8.

The static resolution, R_S, at any point of the panoramic format can be determined from the static resolution versus focus curves and an independent observation of the focus position occupied by the film. In the laboratory, a dynamic film flatness test is performed on each panoramic camera. This test will not be discussed in detail in this report, but the results of the test consist of samples, taken over the panoramic format, of the amount of dynamic film lift above the focal plane rollers (in units of 10^{-3} inch). Actually, the data we are mostly interested in is not the absolute values of film lift but the relative values with respect to the film lift at the center of the format (x = 37.8, y = 2.8). The focus position occupied by the film at the center of the format can be deduced from the dynamic resolution versus focus tests (Figs. 3-7 and 3-9). As previously mentioned, the anticipated air-to-vacuum focus shift was 0.016 inch. So, in Figs. 3-7 and 3-9, the

0 focus setting indicates the anticipated focus position occupied by the film during the mission, assuming a 0.016-inch air-to-vacuum focus shift. Since the actual air-to-vacuum focus shift appears to be only 0.014 inch, we concluded that, during the mission, the film occupied the -2×10^{-3} inch focus positions shown in both Figs. 3-7 and 3-9. Observe that the film positions are 0.002 and 0.001 inch off the peak focus for the aft-looking and forward-looking instruments, respectively, as was mentioned in the Summary. Fig. 3-8 was derived from Fig. 3-7, so the film occupied the -2×10^{-3} inch focus position here also. Comparison of Figs. 3-4 and 3-9 show that the 0 focus setting in Fig. 3-9 should be equal to the -0.1×10^{-3} focus setting in Fig. 3-4. Hence, it was concluded that, during the mission, the film occupied the -2.1×10^{-3} focus setting shown in Fig. 3-4. Using Figs. 3-4 and 3-8 as well as a knowledge of the focus positions of the films during the mission, the static resolutions, R_S, were determined for the center of the format. The static resolution values for any point of the panoramic format were determined as follows:

1. The y distance of the point from the centerline (y = 2.8 centimeters) was determined.

2. This distance, Δy, was converted to a lens field angle, β, by the formula:

$$\beta = \tan^{-1}\left(\frac{\Delta y}{f}\right) \tag{3.14}$$

where f = lens focal length (24 inches)

3. Static resolution versus focus curves (similar to Figs. 3-4 and 3-8) were constructed for the β angle by taking linear interpolations of the corresponding curves of the two nearest field angles for which these curves already exist (0, ±1, ±2, and ±3 degrees).

4. The dynamic film lift, ρ, of the specific point in the format was determined empirically as discussed previously.

5. The film lift at the center of the format, ρ_0, was subtracted from ρ, giving $(\rho - \rho_0)$.

6. Finally, the static resolutions, R_S, were obtained from the corresponding static resolution versus focus curves (from step 3 above) at the focus setting of:

   a. $(-2.1 + \rho - \rho_0) \times 10^{-3}$ inch for unit no. 302
   b. $(-2 + \rho - \rho_0) \times 10^{-3}$ inch for unit no. 303.

This procedure was utilized in determining the static resolution values from which the corresponding dynamic resolutions of the CORN and HPL targets (see Appendices A and B) have been predicted. Each of these targets was analyzed entirely by itself because of the out of focus condition of 1101. The slopes of the low contrast curves at the indicated focus positions of the film during the mission (see Figs. 3-4 and 3-8) are about 40 lines per millimeter and 60 lines per millimeter per 0.001 inch of film lift displacement for unit nos. 303 and 302, respectively. Therefore, film lift is also a critical factor controlling the resolution performance of the 1101 system. Due to the steepness of the resolution curves, large variations in resolution resulted over the panoramic format and between successive frames, which were due to relatively small differences and variations in film lift.

3.2.3 Computation of Image Smear

Image smear results during exposure because the ground image from the Petzval lens moves or has a velocity with respect to the film. This velocity can be separated into two orthogonal

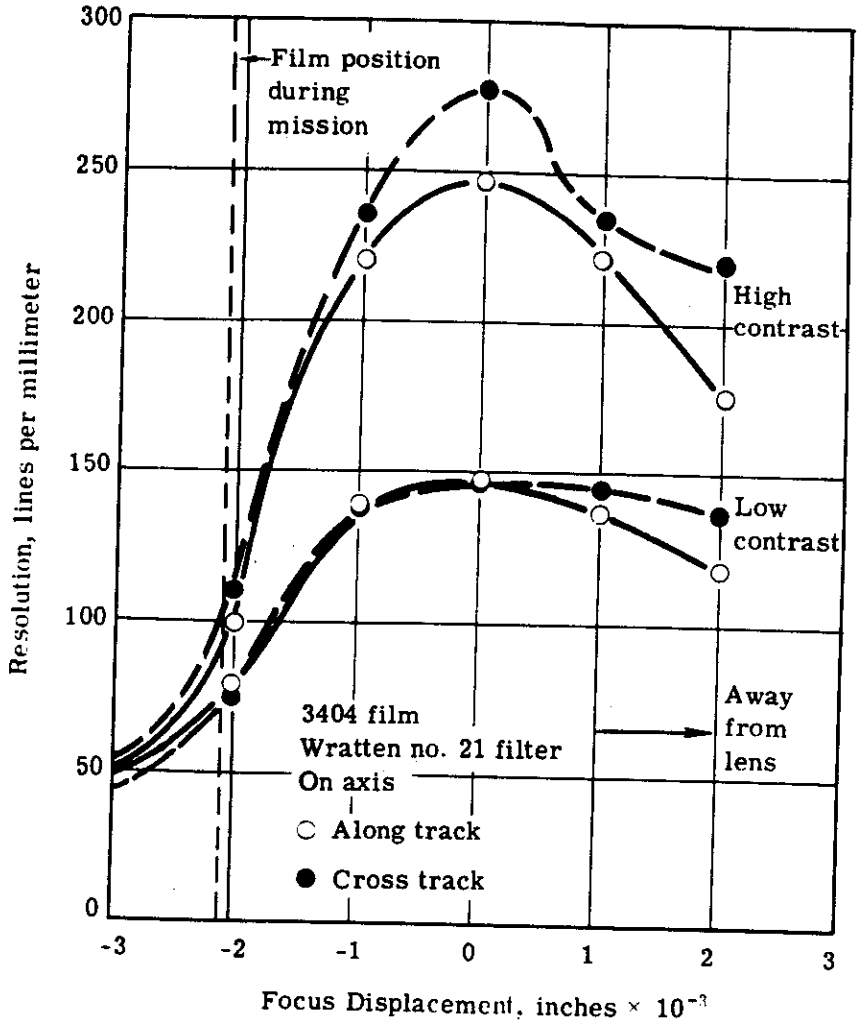

Fig. 3-4 — Unit no. 302 (aft) static resolution versus focus

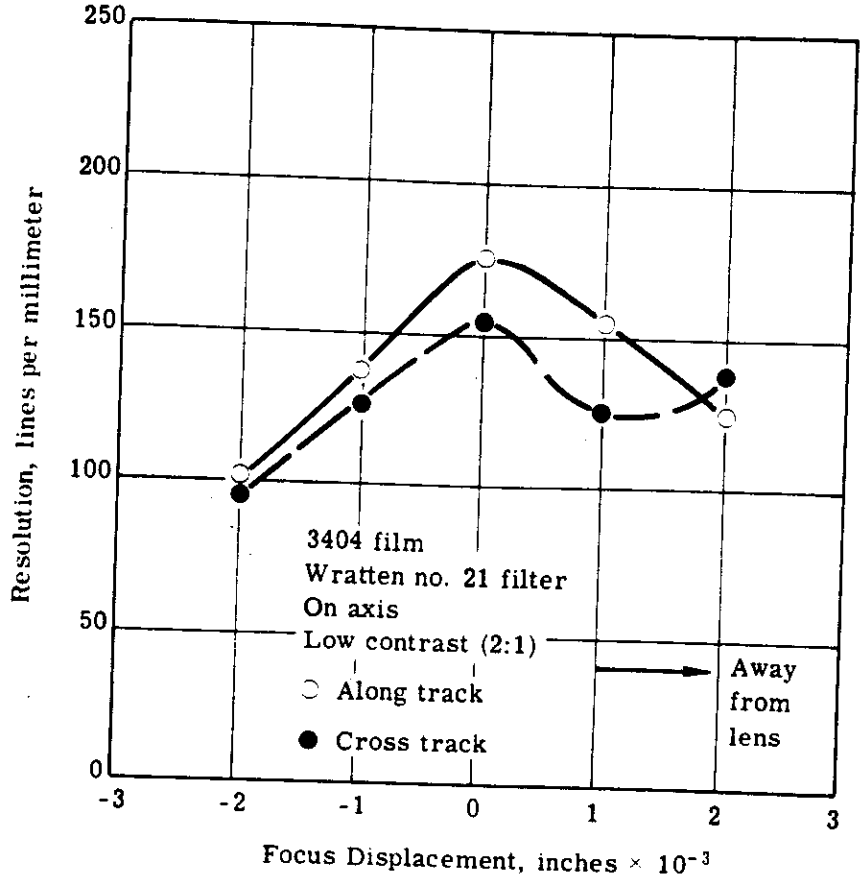

Fig. 3-5 — Unit no. 303 (forward) static resolution versus focus

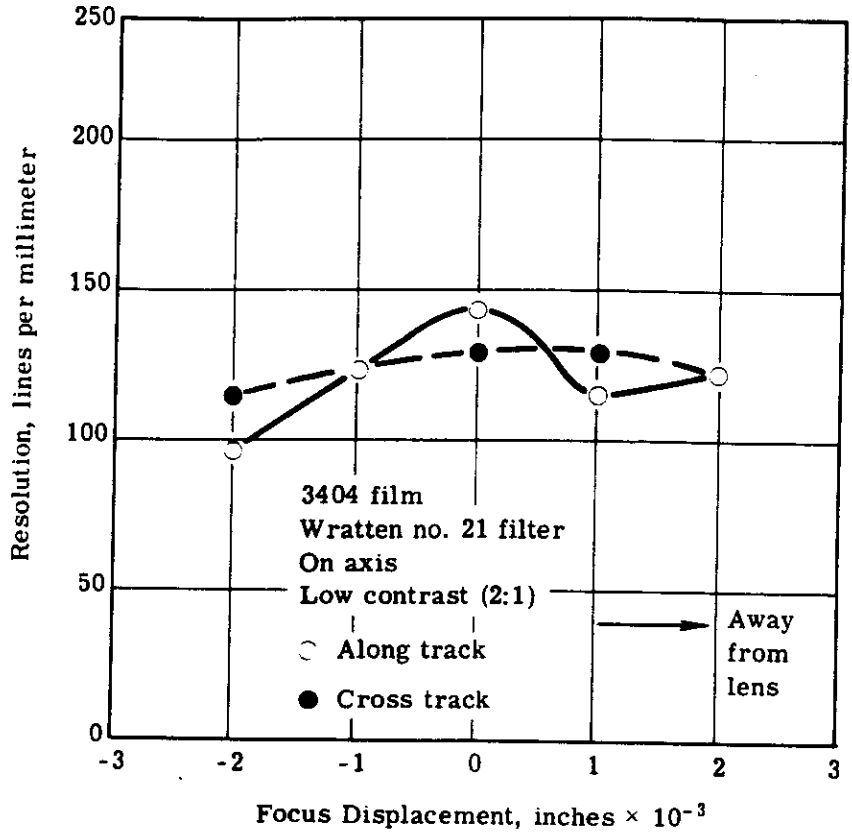

Fig. 3-6 — Unit no. 303 (forward) dynamic resolution versus focus

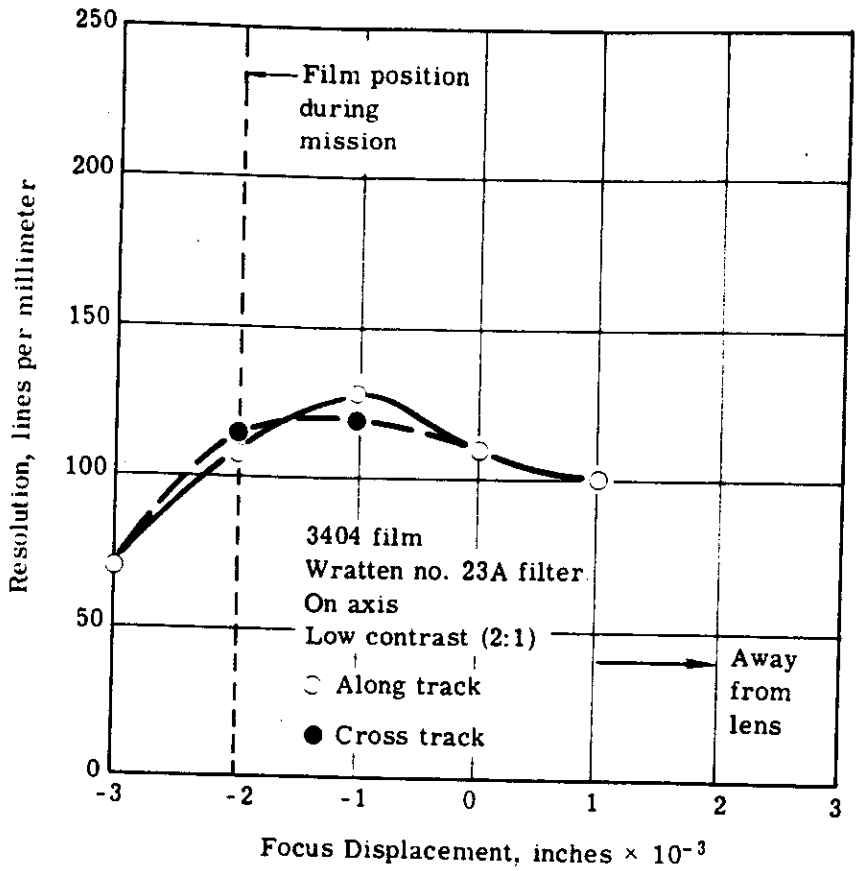

Fig. 3-7 — Unit no. 303 (forward) dynamic resolution versus focus

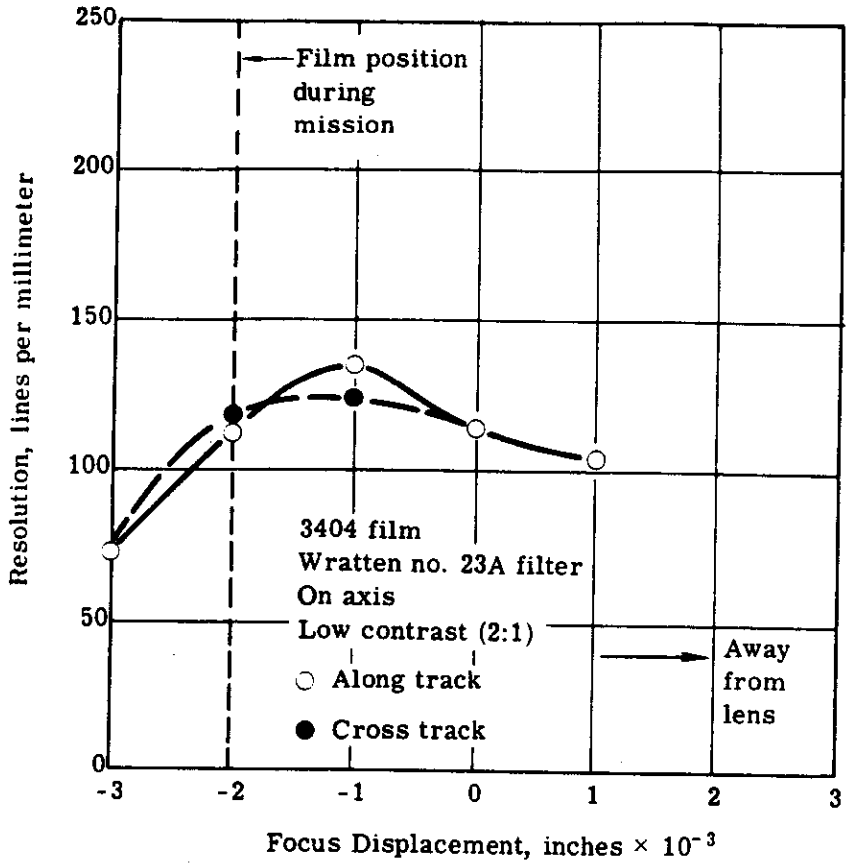

Fig. 3-8 — Unit no. 303 (forward) static resolution versus focus

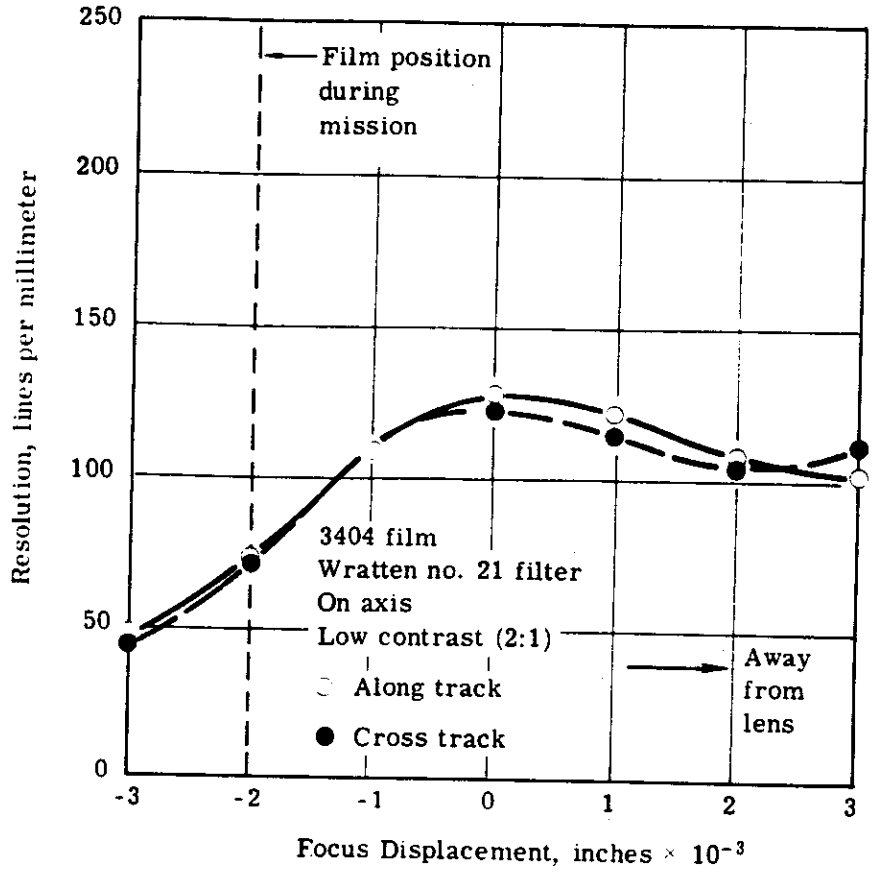

Fig. 3-9 — Unit no. 302 (aft) dynamic resolution versus focus

components, one component in the along-track direction which affects the along-track resolution and the other in the cross-track direction affecting the cross-track resolution. The total image smear in either direction which is the factor b in Equation (3.13) is directly proportional to the exposure time. Table 3-4 shows the major sources of image motion. These sources contribute image motion components which vary over the panoramic format, usually in the predictable manner which depends mainly on the geometry of the panoramic camera and the way ground images are projected on the panoramic format. In general, the total image smear in either direction displays significant variations over the panoramic format. The total image smear also varies with the altitude of the vehicle.

Low altitudes produce larger image smears than high altitudes due to the higher V/h rates and the faster operation of the panoramic cameras at low altitudes. At low altitudes, the dynamic film resolution of a panoramic camera is reduced. However, the reduced scale of the low altitudes more than offsets the loss in dynamic film resolution and the actual ground resolution improves at low altitudes.

In order to determine the total image smear in either direction at a specific point of the panoramic format, the component image smears (see Table 3-4) are computed separately and added. Since there is not enough data to compute all the image smear components from the sources shown in Table 3-4, two image smear values are computed: a systematic image smear, b_S; and a random image smear, b_r. The algebraic sum of all the components whose value and sign (plus or minus) can be established from the available flight data is b_S. On the other hand, b_r is the root-sum-square of all the random components and all the components whose sign is unknown. For each random component, a root-mean-square value was entered. For 1101, all the image smear sources in Table 3-4 identified as Vehicle-Camera Interface Sources and Vehicle Operation Sources produced random components. In addition, the orbital determination error produces a random image motion component. In the along-track direction, the systematic image motion sources (see Table 3-4) were:

1. Uncompensated image motion under camera sources
2. V/h command error.

The other camera sources—vibration, FMC servo error, and FMC cam error—together produce an image smear component of known magnitude (about 1 micron per millisecond of exposure time) but of unknown direction. This component is root-sum-squared with the other random along-track components. In the cross-track direction, the yaw programmer error and all the camera sources listed in Table 3-4 produce systematic image motion components. After b_r and b_S have been computed, the total image smear, b_t, is obtained by adding the magnitudes of b_r and b_S. In other words:

$$b_t = b_r + |b_S| \tag{3.15}$$

In Equation (3.15), b_t becomes a probabilistic quantity. If it is assumed that b_r is the root-mean-square value of a gaussian random variable, then Equation (3.15) means that the probability of the actual image smear being smaller than b_t is between 68 and 84 percent. (If $|b_S| = 0$, the probability is 68 percent; if $|b_S|$ is much greater than b_r, the probability is almost 84 percent.) Obviously, the most accurate determination of the total image smear results when b_r is much smaller than $|b_S|$. Similarly, b_t can be used in Equation (3.13) to compute a dynamic film resolution number. The probability that the actual film resolution is higher than this number is between 68 and 84 percent. In order to compute b_t, the following data from the ephemeris are utilized.

Table 3-4 — Image Motion Sources

Along Track	Cross Track
Camera Sources	**Camera Sources**
Vibration	Vibration
FMC servo error	Film lift
FMC cam error	Lens distortion
Uncompensated image motion	Nodal point error
	Uncompensated cross-track image motion
Command Sources	**Command Sources**
Orbital determination error	Yaw programmer error
V/h command error	
Vehicle-Camera Interface Sources	**Vehicle-Camera Interface Sources**
Roll alignment error	Yaw alignment error
Pitch alignment error	Pitch alignment error
Vehicle Operation Sources	**Vehicle Operation Sources**
Roll attitude error	Roll attitude error
Pitch attitude error	Yaw attitude error
Pitch rate	Pitch attitude error
Yaw rate	Roll rate

1. Vehicle altitude
2. Vehicle velocity
3. Panoramic camera scanning rate
4. Panoramic camera slit width
5. Programmed vehicle yaw angle
6. Required vehicle yaw angle from orbital mechanics.

In addition, the following laboratory data are used:

1. Camera cam constant (the ratio between FMC and scanning rates during format exposure).
2. Along-track camera image smear (about 1 micron per millisecond of exposure time).
3. Cross-track camera image smear (also about 1 micron per millisecond of exposure time). This image motion component has a direction opposite to the direction at which the focal plane rollers scan the panoramic format.

The camera cam constant is nominally 0.01321; however, the cam constant values used in computing b_t were 0.01325 and 0.01315 for unit nos. 302 and 303, respectively. These values were determined by Itek's Data Analysis Center and are part of the panoramic geometry calibration of the 1101 system.

The exposure time is related to the slit width and scanning rate by the following formula:

$$TE = \frac{SLIT}{(SCR)\, f} \tag{3.16}$$

where TE = exposure time
SLIT = slit width
SCR = scanning rate
f = focal length

Also, the FMC rate and scanning rate are related by Equation (3.17):

$$FMC = (CAM)\ SCR \tag{3.17}$$

where FMC = FMC rate
CAM = cam constant discussed above

Actually, the total image smear was calculated in the computer utilizing all the data discussed above. In addition, the computer calculated the film resolutions and the corresponding ground resolutions from the static lens resolutions, R_S, discussed in Section 3.2.2; Equation (3.13); and the parameters, E_1 and E_2, discussed in Section 3.2.1.

The computer program consists of two subroutines. One subroutine allows the computation in either direction (along- or cross-track) of b_t, dynamic film resolution, and ground resolution for any point of the panoramic format by selecting the coordinates, x and y, of the point. The other subroutine allows the computation of the same data for a matrix of 15 points distributed over the panoramic format. This matrix is described in Table 3-5.

The first subroutine has been used to predict resolutions for the CORN and HPL targets (see Appendices A and B).

Table 3-5 — Computational Matrix (θ = scan angle, β = field angle)

θ = -30 degrees β = 2 degrees outboard x = 5.9 y = 0.7	θ = -15 degrees β = 2 degrees outboard x = 21.8 y = 0.7	θ = 0 degrees β = 2 degrees outboard x = 37.8 y = 0.7	θ = +15 degrees β = 2 degrees outboard x = 53.8 y = 0.7	θ = +30 degrees β = 2 degrees outboard x = 69.7 y = 0.7
θ = -30 degrees β = 0 degrees x = 5.9 y = 2.8	θ = -15 degrees β = 0 degrees x = 21.8 y = 2.8	θ = 0 degrees β = 0 degrees x = 37.8 y = 2.8	θ = +15 degrees β = 0 degrees x = 53.8 y = 2.8	θ = +30 degrees β = 0 degrees x = 69.7 y = 2.8
θ = -30 degrees β = 2 degrees inboard x = 5.9 y = 4.9	θ = -15 degrees β = 2 degrees inboard x = 21.8 y = 4.9	θ = 0 degrees β = 2 degrees inboard x = 37.8 y = 4.9	θ = +15 degrees β = 2 degrees inboard x = 53.8 y = 4.9	θ = +30 degrees β = 2 degrees inboard x = 69.7 y = 4.9

3.3 COMPARISON OF CORN TARGETS AND PREDICTED RESOLUTIONS

Table 3-6 shows the static resolutions determined for the CORN targets utilizing their x and y coordinates and the technique and data described in Section 3.2.2. The predicted dynamic CORN target resolutions are shown in Tables 3-7 and 3-8 for unit nos. 303 and 302, respectively. Included in these two tables, for comparison, are the actual CORN target resolutions and their modulations taken from Tables 3-1 and 3-2. The dashes in Tables 3-7 and 3-8 indicate that the data were not available. The CORN targets of pass 16 are not shown in Tables 3-7 and 3-8 because their images were located at the far ends of the panoramic format where film lift undergoes large and unpredictable variations. A few HPL targets were affected by this limitation also. Resolution predictions are missing for a few fixed targets because of a lack of information. In Table 3-7, resolution predictions were not computed for pass 143, frame 20 and pass 173, frame 19, because these CORN targets were photographed with a Wratten no. 25 and no static resolution data are available for this filter. (In the future, these data will be obtained.) In Table 3-8, no resolution predictions were computed for pass 173, frame 25 because this CORN target was photographed with a Wratten no. 23A and no static resolution data are available for this filter either.

In general, it is felt that there is very good agreement between the actual and predicted CORN target resolutions. However, it appears that the following discrepancies exist in Table 3-7:

1. Pass 111, frame 22, cross-track resolution, actual: <59; predicted: 96. This difference might be due to the difference in modulation. The actual modulation was 0.190, while the predicted resolution was for a target modulation of 0.333.
2. Pass 127, frame 15. There seems to be a discrepancy in both along- and cross-track resolutions. However, the actual target modulation is not known. There is a possibility that the differences between actual and predicted resolutions might also be due to the target modulation.
3. Pass 127, frame 23, cross-track resolution. Here, there is a definite discrepancy between actual and predicted resolutions.
4. Pass 157, frame 9, along-track resolution. The actual along-track resolution is unusually high. This can probably be explained by the higher target modulation (0.427 versus 0.333).

The following discrepancies exist in Table 3-8:

1. There is a definite discrepancy on pass 14, frame 37, along-track resolution.
2. Pass 127, frame 19, cross-track resolution. Here the discrepancy is rather small and could be due either to a modulation difference (the actual modulation is unknown) or the fact that the resolution readings were taken from a duplicate positive.
3. There is a definite discrepancy on pass 127, frame 29, for both along- and cross-track directions. This discrepancy can be most likely explained by a dynamic film lift slightly different (possibly less than $5 \cdot 10^{-4}$ inch) than the film lift indicated by the laboratory film flatness test.

3.4 RESOLUTION PREDICTIONS FROM EDGE TARGET ANALYSIS

Modulation transfer functions and resolution predictions have been generated from the edge trace analysis by AFSPPF. This work was performed on a few foreign edge targets listed in the

Edge Target List as well as most of the CORN target displays which contained an edge target. The edge traces as well as the MTF's and resolution predictions were made available to us by AFSPPF. In Tables 3-9 and 3-10 we have entered, for comparison purposes, the predicted resolutions from edge traces of the CORN targets and the actual resolution numbers from the CORN target readings (Tables 3-1 and 3-2).

It is felt that there is no correlation between the resolution numbers generated by the edge trace analysis and the actual CORN target readings. This should be obvious by looking at the numbers in Table 3-9. The resolution numbers generated from edge traces are consistently smaller than those resulting from CORN target readings. The same observation is true about the resolution predictions of Table 3-10, although this table could be misleading because most of the CORN target readings did not produce a definite number but rather an indication that the actual resolution was smaller than a number between 50 and 60 lines. We are convinced that the resolution predictions from edge traces in Table 3-10 are also lower than the actual resolution numbers by about 10 to 15 lines per millimeter. This conclusion was reached because in pass 157, frame 16 (see Table 3-10), the actual cross-track resolution was 56 lines per millimeter. The resolution predicted from the edge trace was 39 lines per millimeter.

The resolution prediction is derived by intersecting the film resolution threshold curve with the MTF computed from the corresponding edge trace. We have tried to improve the resolution predictions by taking into consideration the MTF of the microdensitometer and by using our own film resolution threshold curve discussed in Section 4. However, the improvement in the resolution predictions was minor and indicated that the problem lay with the MTF's derived from the edge traces. Subsequently, we computed our own MTF's from the edge traces. Although our computational technique is quite different from the one AFSPPF uses, the MTF's obtained were very similar. Therefore, it seems that something is wrong with the edge traces, although there is yet no definite explanation or solution to the edge trace MTF problem. We are presently conducting a controlled experiment, trying to correlate MTF's determined by the interferometer method with MTF's obtained from edge traces for the same lens. The results of this test should be quite illuminating and will be available in a separate report.

Table 3-6 — CORN Target Resolutions (lines per millimeter) (Computed)

Forward-Looking Camera, Unit No. 303

		Low Contrast (2:1)		High Contrast	
Pass	Frame	Along Track	Cross Track	Along Track	Cross Track
14	13	93	94		
14	31	101	108		
111	22	93	97		
127	15	93	96		
127	23	108	107		
157	9	93	97		

Aft-Looking Camera, Unit No. 302

14	19	84	91	121	134
14	37	85	77	100	110
111	28	50	53	65	60
127	19	56	61	80	70
127	29	73	67	87	86
143	26	48	41	51	44
143	29	67	57	76	68
157	16	60	56	71	73

Table 3-7 — CORN Target Resolution (lines per millimeter), Comparison of Readings and Predictions, Forward-Looking Camera, Unit No. 303, Low Contrast (2:1)

		Along Track			Cross Track		
			Resolution			Resolution	
Pass	Frame	Modulation	Actual	Predicted	Modulation	Actual	Predicted
14	13	0.427	76	75	0.403	<80	71
14	31	–	88-132	92	0.422	87-130	89
111	22	–	60-80*	80	0.190	<59*	96
127	15	–	88*	78	–	<58*	82
127	23	0.278	75-112	99	0.315	55-73	96
143	20	0.357	76-113	–	0.344	55-73	–
157	9	0.427	116-131	68	0.408	74-112	92
173	19	0.457	74-111	–	0.446	73	–

*From duplicate positive readings.

Table 3-8 — CORN Target Resolution (lines per millimeter), Comparison of Readings and Predictions, Aft-Looking Camera, Unit No. 302

Pass	Frame	Along Track				Cross Track			
		Modulation	Actual Reading	Predicted Low Contrast	Predicted High Contrast	Modulation	Actual Reading	Predicted Low Contrast	Predicted High Contrast
14	19	0.422	< 76	73	93	0.385	< 80	75	94
14	37	–	< 67	76	86	0.315	65-87	72	96
111	28	–	< 58*	50	64	0.329	< 58*	53	60
127	19	–	67*	55	77	–	< 57*	58	66
127	29	0.315	< 57	69	79	0.329	< 55	65	81
143	26	0.365	< 57	47	50	0.375	< 55	41	44
157	16	0.457	< 58	52	59	0.422	56	55	71
173	25	0.417	< 57	–	–	0.474	< 55	–	–

*From duplicate positive readings.

Table 3-9 — Edge Trace Resolutions, Forward-Looking Camera, Unit No. 303, Low Contrast (2:1)

		Along Track			Cross Track		
Pass	Frame	Modulation	Actual Resolution	Predicted Resolution From Edge Trace	Modulation	Actual Resolution	Predicted Resolution From Edge Trace
14	13	0.427	76	122	0.403	<80	55
14	31	–	88-132	–	0.422	87-130	68
127	23	0.278	75-112	48	0.315	55-73	40
143	20	0.357	76-113	45	0.344	55-73	41
157	9	0.427	116-131	51	0.408	74-112	52
173	19	0.457	74-111	–	0.446	73	39

Table 3-10 — Edge Trace Resolutions, Aft-Looking Camera, Unit No. 302, Low Contrast (2:1)

		Along Track			Cross Track		
Pass	Frame	Modulation	Actual Resolution	Predicted Resolution From Edge Trace	Modulation	Actual Resolution	Predicted Resolution From Edge Trace
14	19	0.422	<76	87	0.385	<80	82
14	37	–	<67	–	0.315	65-87	101
16	11	0.301	102	59	0.245	<91	53
127	29	0.315	<57	32	0.329	<55	34
143	26	0.365	<57	39	0.375	<55	43
157	16	0.457	<58	35	0.422	56	39
173	25	0.417	<57	38	0.474	<55	42

4. A TAKEUP EXPERIMENT

4.1 GENERAL

The A takeup experiment, so named because the film investigated is located in the A takeup bucket, was undertaken to define the image quality of the mission emulsion batch of type 3404 film.

The experiment consisted of a comparison of image quality on samples of type 3404 film. Film resolution (AIM curves), granularity (rms), and film modulation transfer (MTF) were the areas investigated. The image quality of the flight film was reported as a function of specific environmental conditions. The film samples were classified as follows:

1. Control: current process control for 3404 film (3404-277).
2. Preflight control: refrigerated film of the same emulsion batch used in the mission.
3. A takeup: film run through the camera prior to launch and removed from the recovery capsule prior to processing.

Using daylight and a Wratten no. 23A filter, resolving power targets (resolution), edges (MTF), and flashed density patches (granularity) were exposed on the film samples and the samples were then processed with the mission film.

4.2 FILM RESOLUTION—AIM CURVE DERIVATION

Using replicated exposure series target readings, resolution was established at five contrast levels. The strip configuration, data reduction, resultant AIM curves, and an analysis of variance was performed on the three different film conditions. No significant difference was found between the control, preflight control, and the A takeup film samples. This was concluded from an analysis of variance comparing the variance from film to film with that associated with establishing single resolution values.

Strips for the six contrasts (consisting of three exposure series of 11 steps read from high to low density by three readers) were produced and read for control (3404-277), preflight control (3404-292), and A takeup samples (3404-292).

Three targets were read by three readers for each exposure level, giving 9 group/element readings. These readings were made for all 11 exposure levels giving a total number of 99 group element readings per contrast. The group/element readings were then converted to log resolution values for further analysis. The nine log resolution values for each of the 11 exposure levels were averaged to yield 11 average log resolution values as a function of exposure. Because film resolution is considered to be the maximum read from a strip at whatever exposure produces it, the highest log resolution value was chosen from the series as representative of the film resolution for that strip or contrast level.

Based on the estimated mean and the variance associated with the nine readings used to estimate the mean, 95 percent confidence limits were established about the true mean. The 95 percent confidence limits, found in log form and converted to linear values, establish limits within which the true film resolution could be expected to lie 95 percent of the time. Table 4-1 lists the results of this reduction.

AIM curves were drawn from the reduced data for control, preflight control and A takeup conditions. Modulation was plotted against resolution to produce each AIM curve. Thus, the final product of all of the data reduction consists of the three AIM curves shown in Figs. 4-1, 4-2, and 4-3.

In order to compare the three film samples, an analysis of variance was performed to determine whether or not there was a significant difference between the film resolutions. It was inferred, from this analysis, that there was no significant difference between the three film resolutions at the alpha equals 0.05 level of significance.

The experimental design consisted of a two-variable repeated measurement experiment. The two variables were the three films and the five contrast levels. The repeated measurements were the nine readings for each strip that yielded the highest average resolution. F values were computed from the mean square for the film, with the contrast level and residual all being compared to the within-groups variance. The contrast levels were found to yield different resolutions as expected; however, no significant difference was found between films.

4.3 RMS GRANULARITY

The rms granularity values were determined at four density levels for the control, preflight control, and A takeup film samples. The resulting curves (granularity as a function of density) and the granularity values at the 1.0 gross density level are reported herein (refer to Fig. 4-2 and Table 4-2). The curves representing the preflight control and A takeup samples show what might be a significant difference. It is hoped that the information from the next mission will enable us to determine if this apparent difference exists and, if so, if it is significant.

The aperture size, 12 microns, was chosen as a result of discussion and agreement between Itek and Eastman Kodak personnel, as it was considered to be more in keeping with the viewing magnification to be used on the system product. To convert reported rms values thus determined to figures comparable to those obtained with a 24-micron aperture size, divide the values by two in conformance with Selwyn's Law.

Aperture size	12 ± 1 micron
Data point spacing	Approximately 10 percent diameter overlap
Number of density patches per strip	4
Number of scans per density patch	5
Number of data points per scan	500

The rms granularity values were computed for each of 60 scans using bad data point elimination and detrending techniques. A pooled estimate of the variance and rms value was calculated for each patch. These are shown with 95 percent confidence limits about the rms value (see Fig. 4-4). The Chi-square distribution was used to compute these limits. The rms values at 1.0 gross density are presented in Table 4-2.

It would be preferable to have a 1.0 gross density patch, since any statistical comparison between films at the 1.0 level requires an empirical measure of granularity taken from a 1.0 density patch rather than an interpolated value using rms values at about 0.8 and 1.2 gross density.

4.4 FILM MODULATION TRANSFER FUNCTION

The modulation transfer functions (MTF) of type 3404 film for the control, preflight control, and A takeup samples exposure conditions were compared and are shown in Fig. 4-5. The Eastman Kodak calculated curve for 3404 is included for comparison. Note that the manufacturer's curve is lower than the estimate of the MTF. There are several reasons why this occurred; the most prevalent one is that the measurement techniques are different. The Eastman Kodak published curve was determined from sinusoids, ours from edges. It is believed that using edges is fundamentally better from a system engineering standpoint since this technique is used in determining operational MTF's and the two are therefore compatible. The difference encountered here is not considered to be important since the control batch (which is the same type as used for the EK data) was used in our test and it is not significantly different from the other two curves. The MTF's were calculated incorporating edge traces made at AFSPPF and Itek's computation techniques. A comparison of the Itek and AFSPPF MTF programs was made, and there is apparently no statistical difference between the two methods. The MTF calculations include the MTF's of the following:

1. Microscope camera optics
2. Film
3. Process.

The microdensitometer MTF was removed from the resultant curves. These functions are all reported as film MTF's because it is felt that the two remaining factors, namely the microscope camera optics and the process, result in insignificant changes in the MTF. The MTF's from each of the three conditions is an average of five individually calculated functions with confidence limits of 95 percent placed around the curves. It is evident that there is no significant difference between the three conditions.

Table 4-1 — Results of Data Reduction

Filter	Identification Source	Target* Contrast	Target Modulation	Resolution, lines per millimeter 1-Sigma Range Average	From	To
78 + 23A	Control (3404-277)	1.28:1	0.1228	143	134	153
78 + 23A	Control (3404-277)	1.70:1	0.2592	221	205	238
78 + 23A	Control (3404-277)	1.95:1	0.3220	300	284	316
78 + 23A	Control (3404-277)	2.63:1	0.4490	328	305	353
78 + 23A	Control (3404-277)	5.14:1	0.6743	413	393	434
78 + 23A	Preflight control (3404-292)	1.28:1	0.1228	141	124	160
78 + 23A	Preflight control (3404-292)	1.70:1	0.2592	264	240	290
78 + 23A	Preflight control (3404-292)	1.95:1	0.3220	300	278	323
78 + 23A	Preflight control (3404-292)	2.63:1	0.4490	328	308	349
78 + 23A	Preflight control (3404-292)	5.14:1	0.6743	413	399	427
78 + 23A	A takeup (3404-292)	1.28:1	0.1228	156	146	167
78 + 23A	A takeup (3404-292)	1.70:1	0.2592	248	238	257
78 + 23A	A takeup (3404-292)	1.95:1	0.3220	257	241	275
78 + 23A	A takeup (3404-292)	2.63:1	0.4490	320	303	338
78 + 23A	A takeup (3404-292)	5.14:1	0.6743	413	399	427

*Future reports will utilize different target contrast to encompass a wider range of modulations.

Table 4-2 — RMS (12-Micron) Granularity at 1.0 Gross Density

Control (3404-277)	0.036
Preflight control (3404-292)	0.034
A takeup (3404-292)	0.038

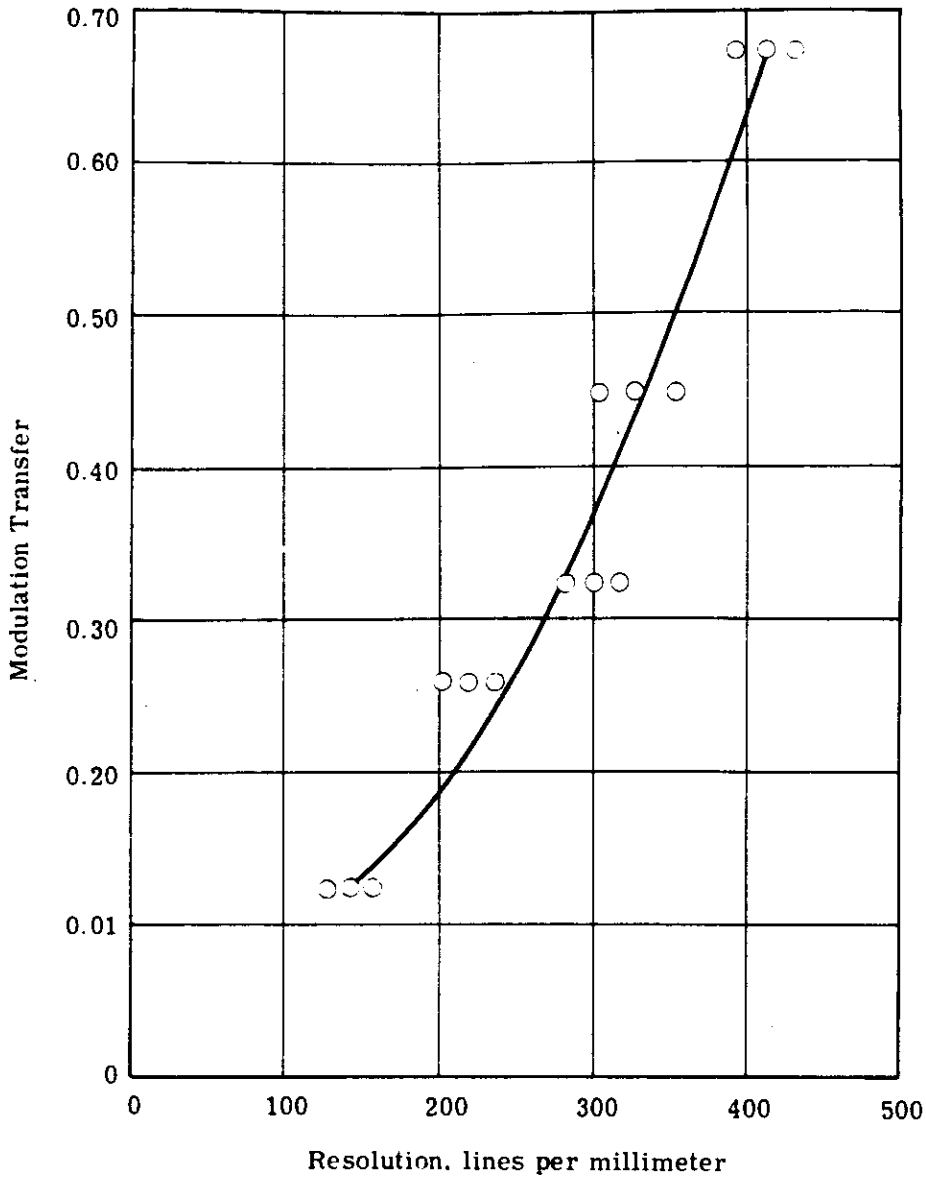

Fig. 4-1 — Test object modulation versus resolution (AIM) for the control film sample

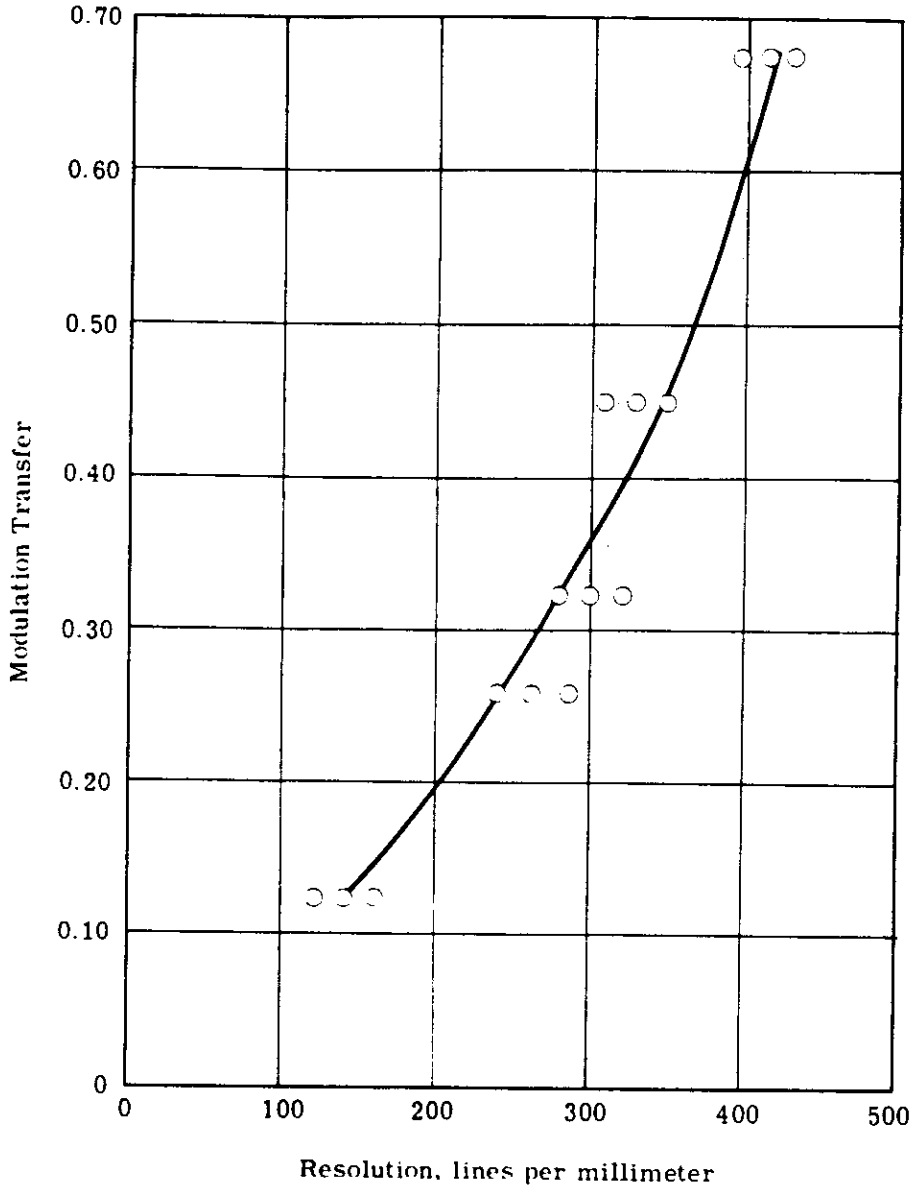

Fig. 4-2 — Test object modulation versus resolution for the preflight control film sample

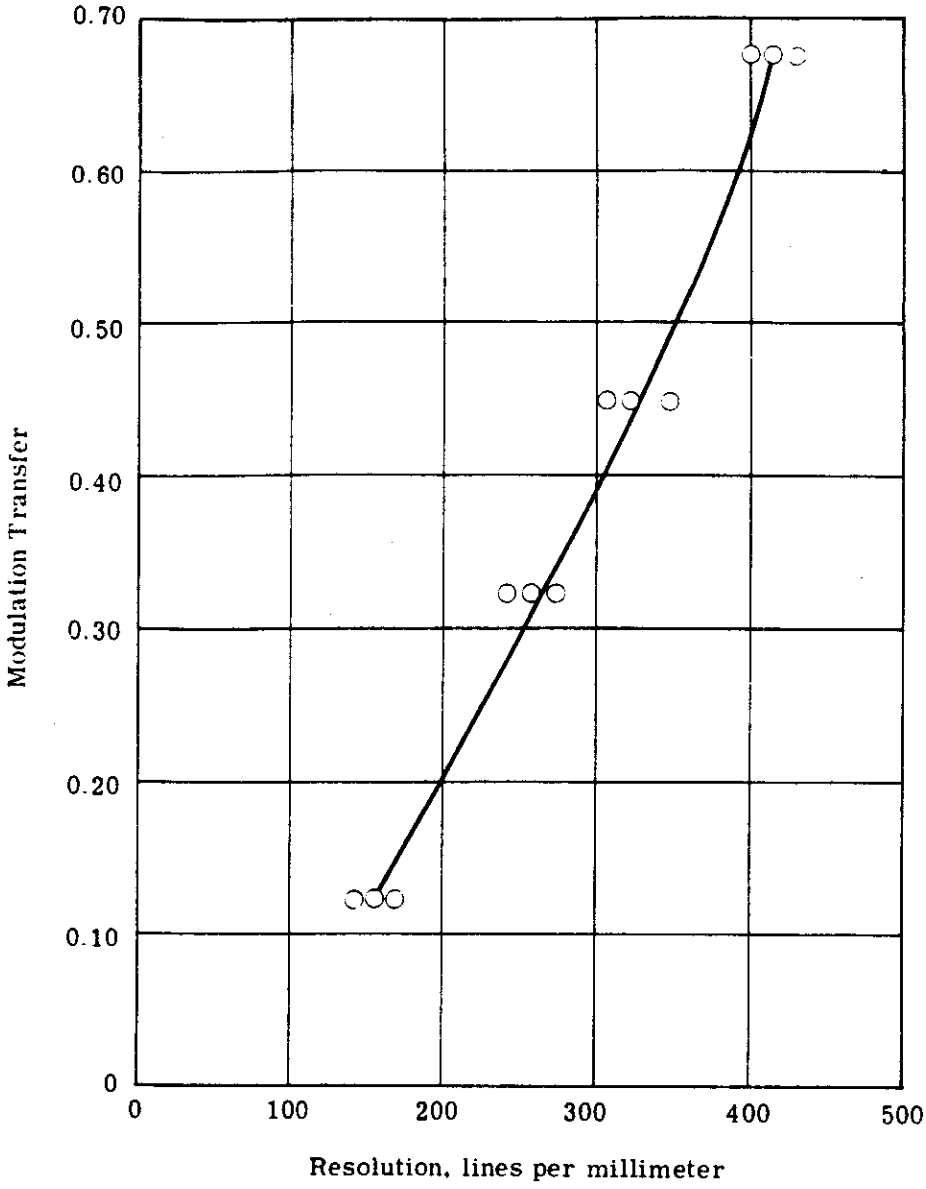

Fig. 4-3 — Test object modulation versus resolution for the A takeup film samples

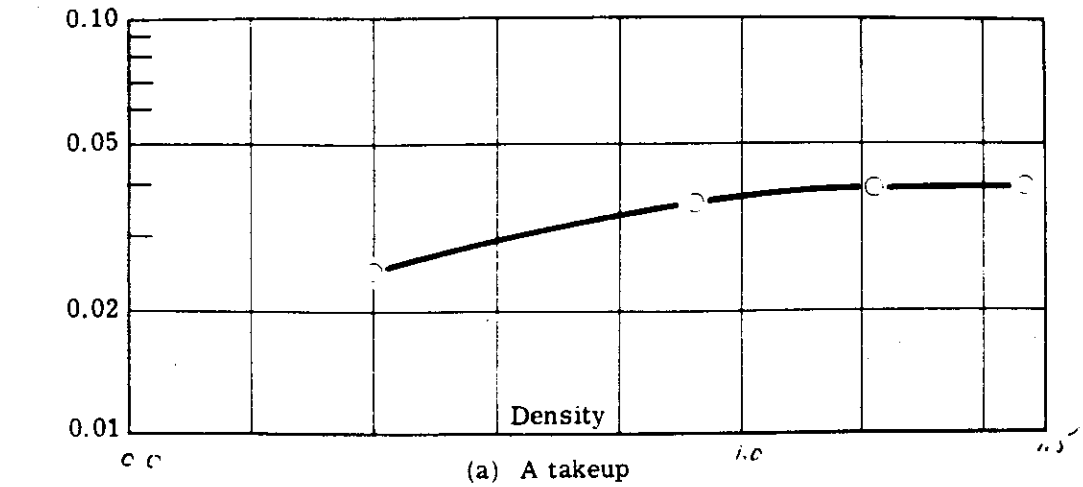

(a) A takeup

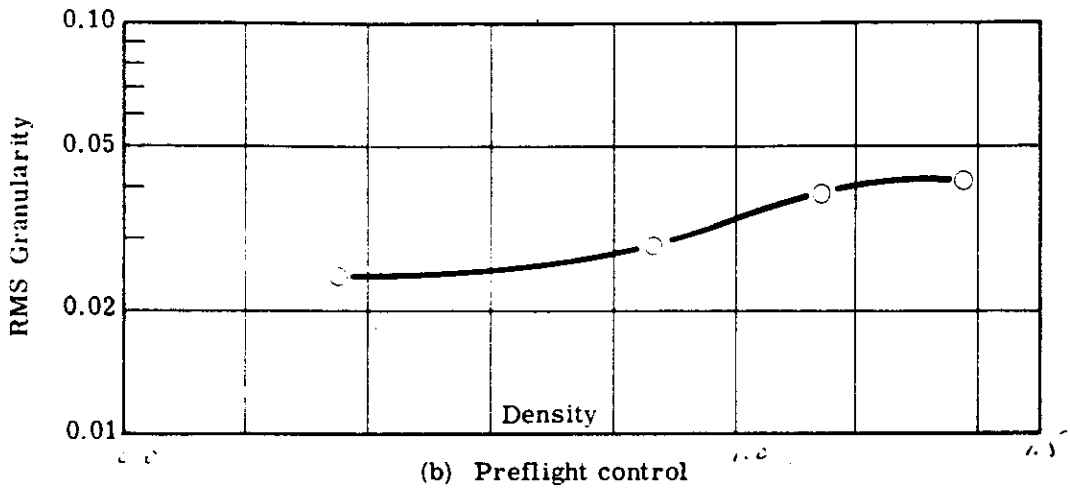

(b) Preflight control

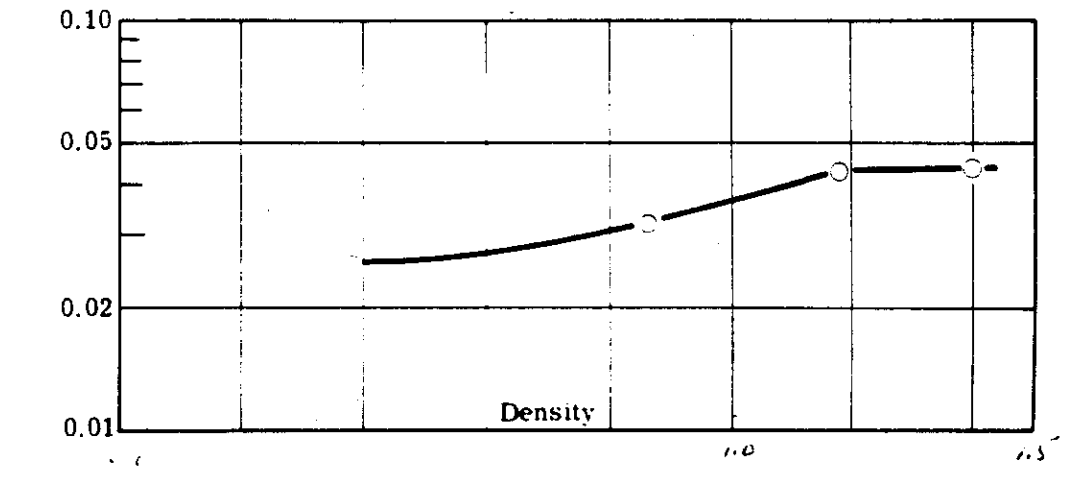

(c) Control

Fig. 4-4 — Granularity of film samples as a function of density

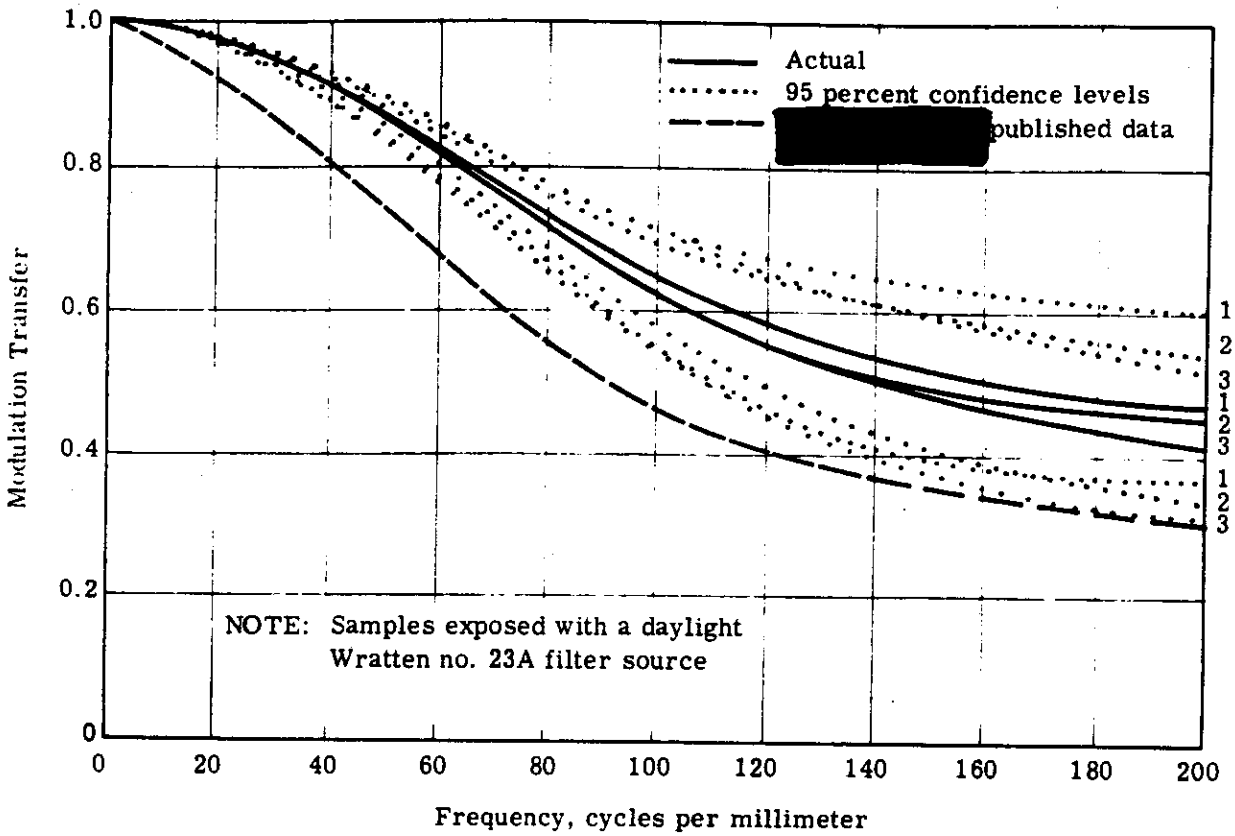

Fig. 4-5 — MTF of type 3404 film

5. DENSITY ANALYSIS

5.1 OBJECTIVE

The objective of the density analysis was to determine if the 1101 mission film was properly exposed. To do this, a series of COMIREX Priority I targets was evaluated. In the past, the [redacted] terrain measurements have been used to make this judgment; however, investigation reveals that a serious drawback is associated with the use of this criterion. Because the densities are made from a random sampling of frames, some may be of no importance to the photointerpreter. The target measurements, on the other hand, are made of prime areas of interest and if these targets are properly exposed, the mission as a whole should be so judged.

The targets were scanned with a microdensitometer, and the minimum and maximum densities of these traces were evaluated in terms of their location in the D-log E curve of the mission emulsion. The target minimum and maximum densities were then compared with the [redacted] terrain density measurements to ascertain whether a correlation exists between the two units.

5.2 PROCEDURE

A single microdensitometer scan was made across the COMIREX Priority I targets. The scanning aperture was 10 microns in diameter, representing 8 to 10 feet on the ground. The traced area was chosen to cover the portions of the target which are of greatest interest to the photointerpreter. The traces were subjectively analyzed to determine the minimum and maximum densities. Fig. 5-1 shows an example of how this judgment was made. Note that point "A" is not consistent with the other minimum density areas and is therefore not considered in the analysis. These densities and their corresponding pass, frame, camera, target number, slit, and filter are shown in Table 5-1.

The criterion for judging the exposure quality of a target is based on the film's characteristic curve. The minimum density should fall in an area of the curve where small exposure differences will be recorded as significant density differences. The maximum density should follow the same criterion, and at the same time not be so high an exposure as to produce excessive light scattering within the emulsion. For 3404 film it has been decided that a minimum density below 0.4 is an underexposed condition and a minimum density above 0.8 or a maximum density above 2.0 is an overexposed condition.

The terrain densities as determined by [redacted] are shown in Table 5-2. The terrain measurements were made with a densitometer having a 0.5-millimeter spot aperture. The measured frames were chosen at random and the sample size was statistically determined so that a valid judgement could be made concerning the total mission. The mission was divided into four portions (the first and second buckets of the forward and aft cameras) and the total average minimum and maximum densities for each section are reported in Table 5-2.

Table 5-1 — Density Analysis

Pass	Frame	Camera	Target[1]	Slit	Filter	D_{min}	D_{max}
D-008	004	Fwd	704	0.272	W-23A	0.28[2]	0.86
D-008	012	Aft	704	0.225	W-21	0.34[2]	1.00
D-037	006	Fwd	119	0.272	W-23A	0.58	1.14
D-037	013	Aft	119	0.225	W-21	0.75	1.38
D-196	010	Fwd	119	0.218	W-23A	0.43	1.28
D-196	016	Aft	119	0.175	W-21	0.62	1.18
D-040	018	Fwd	105	0.272	W-23A	0.43	1.34
D-054	004	Fwd	117	0.272	W-23A	0.60	1.65
D-054	010	Aft	117	0.225	W-21	0.83	1.65
D-056	106	Fwd	125	0.272	W-23A	0.49	1.37
D-056	112	Aft	125	0.225	W-21	0.62	1.76
D-071	006	Fwd	114	0.272	W-23A	0.50	1.02
D-071	013	Aft	114	0.225	W-21	0.70	1.14
D-071	044	Fwd	124	0.272	W-23A	1.04[3]	1.61
D-071	050	Aft	124	0.225	W-21	1.28[3]	1.78
D-072	053	Fwd	108	0.272	W-23A	0.40	1.24
D-072	059	Aft	108	0.225	W-21	0.32[3]	1.32
D-088	027	Fwd	108	0.272	W-23A	0.40	1.53
D-088	034	Aft	108	0.225	W-21	0.45	1.50
D-072	059	Fwd	113	0.272	W-23A	0.50	1.32
D-072	065	Aft	113	0.225	W-21	0.44	1.43
D-088	032	Fwd	113	0.272	W-23A	0.35[4]	1.29
D-088	039	Aft	113	0.225	W-21	0.39[4]	1.23
D-086	005	Fwd	109	0.272	W-23A	0.46	1.47
D-086	011	Aft	109	0.225	W-21	0.58	1.70
D-132	012	Fwd	106	0.272	W-23A	0.46	1.11
D-132	018	Aft	106	0.225	W-21	0.51	1.11
D-136	043	Fwd	118	0.272	W-23A	0.78	1.32
D-182	010	Fwd	111	0.272	W-23A	0.53	0.97
D-182	016	Aft	111	0.225	W-21	0.54	1.14
D-199	065	Fwd	101	0.272	W-23A	0.22[5]	0.64
D-199	071	Aft	101	0.225	W-21	0.26[5]	0.70

[1]Arbitrary number assigned for the purpose of this study by NPIC.
[2]The low D_{min} is a result of a micro-d scan across a waterway.
[3]The high D_{min} and D_{max} are produced from a scene having blowing snow.
[4]The low D_{min} is a result of a scan across the trees.
[5]This scene is underexposed.

Table 5-2 — [redacted] Terrain Densities

Mission	Camera	D_{min}	D_{max}
1101-1	Fwd	0.45	1.0
1101-1	Aft	0.61	1.20
1101-2	Fwd	0.50	1.08
1101-2	Aft	0.45	1.10

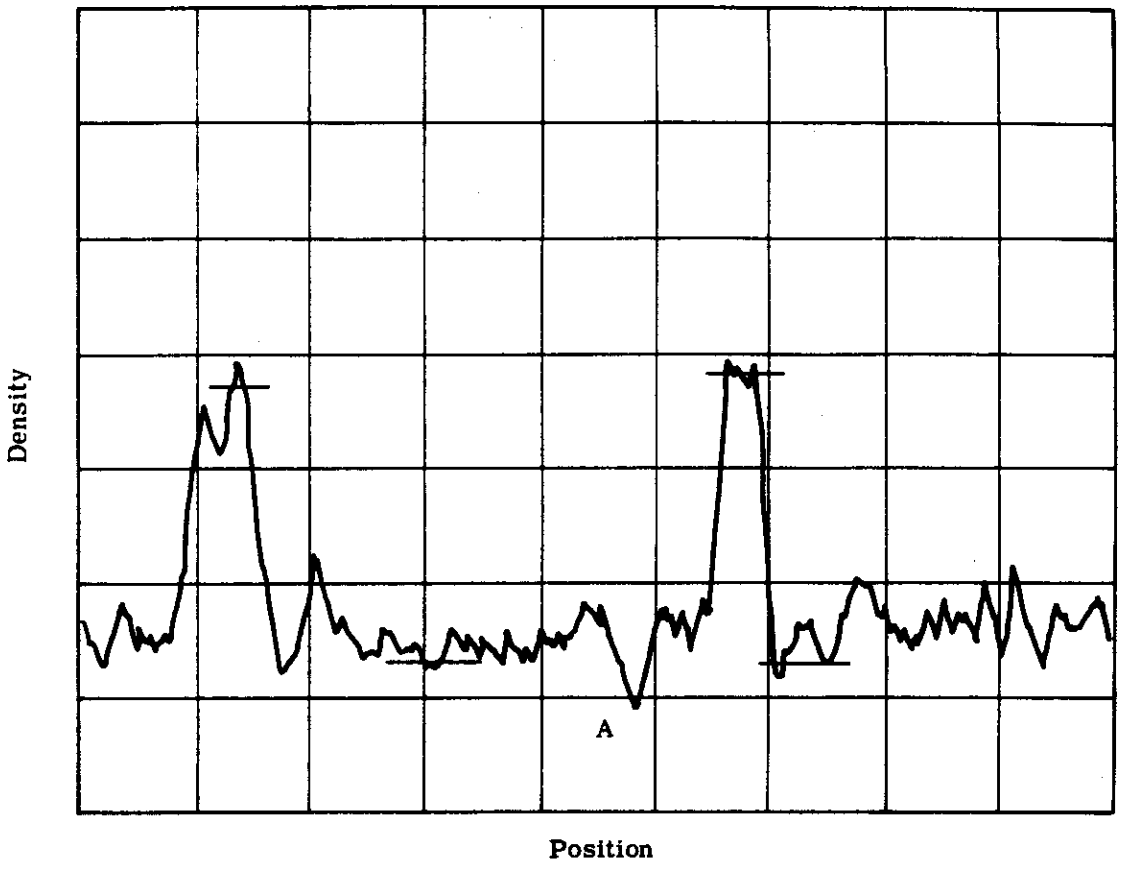

Fig. 5-1 — Sample of a microdensitometer scan of a COMIREX Priority I target

5.3 RESULTS

An examination of the minimum and maximum densities in Table 5-1 indicated that of the 32 targets traced, both portions of passes D-008, D-088, and D-199 and one portion of pass D-072 have minimum densities below the judgment criterion for an underexposed condition. Both portions of pass D-071 meet the overexposure criterion.

These under- and overexposed conditions can generally be explained by examining the particular target type or its surrounding area. In some instances, the object adjacent to the target, but not directly associated with it (the dark trees of passes D-072 and D-088 or the water of pass D-008), produced the very low densities. Likewise, the blowing snow on pass D-071 produced a very high minimum density. It is not known whether these conditions warrant a valid judgment of an under- or overexposed condition. There is no such explanation associated with pass D-199, and it is believed that this target is underexposed.

The minimum densities from the COMIREX Priority I targets and the terrain measurements are shown in Table 5-3. It is significant to note, that of the 32 cases, the targets had a lower minimum density 14 times or 43 percent, and the terrain measurements were lower 17 times or 57 percent. Therefore, the target and terrain measurements were split almost 50/50 as far as which had the lower minimum density.

5.4 CONCLUSION

Generally, the exposure of the COMIREX Priority I targets was acceptable. If the analyses were performed irrespective of the weather conditions or surrounding area, seven or 19 percent of the targets are underexposed and two or 6 percent are overexposed; the remaining 75 percent are well exposed.

There is insufficient data at this time to make a valid comparison between the target and terrain densities. Three targets, nos. 119, 108, and 113, were photographed on two different passes. In no instance was any of these consistently over- or underexposed.

Table 5-3 — Target D_{min} Versus Terrain D_{min}

Target	Terrain	Target	Terrain	Target	Terrain	Target	Terrain
0.28	0.45	0.32	0.61	0.83	0.61	0.58	0.45
0.34	0.61	0.40	0.50	0.49	0.45	0.46	0.50
0.58	0.45	0.45	0.45	0.62	0.61	0.51	0.45
0.78	0.61	0.50	0.45	0.50	0.45	0.78	0.50
0.43	0.50	0.44	0.61	0.70	0.61	0.53	0.50
0.62	0.45	0.35	0.50	1.04	0.45	0.54	0.45
0.43	0.45	0.39	0.45	1.28	0.61	0.22	0.50
0.60	0.45	0.46	0.50	0.40	0.45	0.26	0.45

6. RECOMMENDATIONS

As a result of the information acquired and the findings of the 1101 systems analysis work, the following recommendations are made:

1. The CORN target displays should be re-examined. As discussed in Section 3.1, at least five targets are needed between the 8- and 16-foot targets.

2. The various dynamic resolution versus image smear tests that have been run to date showed that the peak focus position of each camera should be determined from experimental resolution versus image smear curves that are obtained at various focus positions. The dynamic focusing technique utilized on 1101, 1102, and 1103 could produce peak focus errors as large as 0.001 inch.

3. In computing the dynamic camera resolution, the following equation should be used:

$$R_d = \frac{R_S}{[1 + (bR_S)^{E_1}]^{E_2}}$$

where R_d = dynamic camera resolution
R_S = static lens/film resolution
b = image smear
E_1 and E_2 = experimentally determined exponents (see Section 3.2.1)

These exponents depend on the lens performance, and should be determined individually for each lens.

4. The apparent failure of the edge target analysis to produce reasonable MTF's should be investigated further. Presently, MTF tests are being performed on two Petzval lenses that will permit a comparison between the MTF's of the lenses, determined by the unequal path interferometer (UPI), and the MTF's of the same lenses determined by edge trace analysis.

5. The criterion for exposure should not be changed. This recommendation is based only on the density analysis of the HPL targets covered by the 1101 system. However, evaluation of future systems may reveal some difficulties with the present exposure criterion.

6. We strongly recommend that the resolution predictions of the HPL targets appearing in Appendix B be empirically correlated with the sizes and types of objects that can be recognized by the photointerpreters. The predicted average ground resolutions and the photointerpreter's ratings of certain HPL targets identified by NPIC members have been entered for comparison in Table B-3 of Appendix B. From this table, it appears that there is excellent correlation between photointerpreter's ratings and predicted average ground resolution.

7. Subsequent tests (1102 mono operation) validated the high performance capability of this mode. Therefore, it is recommended that a study be made to effect the disabling of a failed instrument to save power and enable mono operation for the unfailed instrument.

Appendix A

RESOLUTION PREDICTIONS FOR CORN TARGETS

This appendix is a listing of the image smear and resolution data which have been computed for the CORN targets (see Tables A-1 and A-2).

Notation

BALTR = image smear, along track, random, microns

BALTS = image smear, along track, systematic, microns

TBAT = total blur, along track, microns

RESL = dynamic film resolution, along track, low contrast (2:1), lines per millimeter

RESH = dynamic film resolution, along track, high contrast, lines per millimeter

GDRL = ground resolution, along track, low contrast, feet

GDRH = ground resolution, along track, high contrast, feet

BCTR = image smear, cross track, random, microns

BCTS = image smear, cross track, systematic, microns

TBCT = total image smear, cross track, microns

CRESL = dynamic film resolution, cross track, low contrast, lines per millimeter

CRESH = dynamic film resolution, cross track, high contrast, lines per millimeter

CGDRL = ground resolution, cross track, low contrast, feet

CGDRH = ground resolution, cross track, high contrast, feet

x = x coordinate of target, centimeters

y = y coordinate of target, centimeters

ROL = static film resolution, along track, low contrast, lines per micron

ROH = static film resolution, along track, high contrast, lines per micron

RCL = static film resolution, cross track, low contrast, lines per micron

RCH = static film resolution, cross track, high contrast, lines per micron

Table A-1 — Resolution Predictions for CORN Targets, Forward-Looking Camera, Unit No. 303

Pass	14	14	111	127	127	157
Frame	13	31	22	15	23	9
Along Track						
BALTR	3.20	3.21	3.21	3.21	3.21	4.01
BALTS	3.63	0.63	2.23	2.70	-0.20	4.41
TBAT	6.83	3.84	5.44	5.91	3.41	8.42
RESL	74.6	92.2	80.2	78.3	99.4	68.2
RESH	–	–	–	–	–	–
GDRL	16.3	11.5	12.0	12.1	9.0	13.7
GDRH	–	–	–	–	–	–
Cross Track						
BCTR	0.58	0.65	0.65	0.65	0.67	0.82
BCTS	7.27	4.72	0.35	4.68	3.31	2.13
TBCT	7.85	5.38	1.00	5.33	3.98	2.95
CRESL	70.9	89.4	96.4	82.5	96.0	92.2
CRESH	–	–	–	–	–	–
CGDRL	18.1	11.7	9.8	11.3	9.1	9.7
CGDRH	–	–	–	–	–	–

Table A-2 — Resolution Predictions for CORN Targets, Aft-Looking Camera, Unit No. 302

Pass	14	14	111	127	127	143	143	157
Frame	19	37	28	19	29	26	29	16
Along Track								
BALTR	2.57	2.58	2.58	2.58	2.58	1.97	2.51	3.31
BALTS	3.26	2.37	0.01	0.23	1.72	1.07	1.25	4.88
TBAT	5.28	4.94	2.59	2.81	4.30	3.05	3.76	8.19
RESL	73.1	76.5	49.5	55.1	68.7	47.3	64.4	52.1
RESH	93.2	86.4	63.7	77.2	79.5	50.1	71.9	58.6
GDRL	16.6	14.0	18.7	16.7	13.3	19.2	15.2	17.8
GDRH	13.0	12.4	14.5	11.9	11.5	18.1	13.6	15.9
Cross Track								
BCTR	0.46	0.52	0.52	0.52	0.53	0.41	0.47	0.67
BCTS	5.96	3.88	0.35	3.92	2.70	2.22	5.16	1.82
TBCT	6.43	4.40	0.87	4.44	3.24	2.63	5.63	2.49
CRESL	75.2	71.8	52.9	58.3	65.0	40.7	53.5	55.3
CRESH	94.1	95.5	59.9	65.6	81.5	43.5	61.9	71.2
CGDRL	17.1	14.6	17.5	15.7	13.6	21.6	19.2	16.1
CGDRH	13.6	11.0	15.4	14.0	10.8	20.2	16.6	12.5

Appendix B

RESOLUTION PREDICTIONS FOR HPL TARGETS

Resolution predictions for HPL targets are contained in Tables B-1 and B-2. Table B-3 contains data concerning average low contrast ground resolution versus the photointerpreter's rating.

Table B-1 — Resolution Predictions for HPL Targets, Forward-Looking Camera, Unit No. 303

Target	119	117	125	114	124	108	113	109
Pass	37	54	56	71	71	72	72	86
Frame	6	4	106	6	44	53	59	5
X	41.4	31.2	22.7	52.4	12.1	32.9	10.2	46.6
Y	0.5	3.2	4.6	1.1	3.6	5.1	3.9	4.4
ROL	0.093	0.103	0.105	0.091	0.114	0.092	0.111	0.088
ROH	–	–	–	–	–	–	–	–
RCL	0.094	0.104	0.116	0.094	0.107	0.109	0.104	0.101
RCH	–	–	–	–	–	–	–	–
Along Track								
BALTR	4.01	4.01	4.00	4.00	3.99	4.01	3.99	4.01
BALTS	4.29	1.69	0.44	4.07	2.28	0.92	0.77	-0.14
TBAT	8.30	5.70	4.44	8.08	6.27	4.93	4.76	4.15
RESL	68.7	85.0	92.4	68.7	87.2	81.5	94.6	81.1
RESH	–	–	–	–	–	–	–	–
GDRL	16.5	13.2	11.8	16.8	13.3	14.0	13.3	13.1
GDRH	–	–	–	–	–	–	–	–
Cross Track								
BCTR	0.83	0.83	0.80	0.80	0.73	0.83	0.72	0.83
BCTS	4.75	2.71	0.83	6.97	-1.24	3.25	-1.22	5.74
TBCT	5.58	3.54	1.63	7.77	1.97	4.08	1.94	6.57
CRESL	80.3	95.8	113.4	71.2	104.0	96.9	101.3	79.7
CRESH	–	–	–	–	–	–	–	–
CGDRL	13.5	11.4	9.7	16.0	11.7	11.5	13.4	13.2
CGDRH	–	–	–	–	–	–	–	–

Table B-1 — Resolution Predictions for HPL Targets, Forward-Looking Camera, Unit No. 303 (Cont.)

Target	108	113	118	111	101
Pass	88	88	136	182	199
Frame	27	32	43	10	65
X	66.2	49.6	66.1	63.5	18.8
Y	1.7	2.6	5.0	3.9	4.7
ROL	0.089	0.099	0.075	0.110	0.101
ROH	–	–	–	–	–
RCL	0.087	0.105	0.089	0.102	0.114
RCH	–	–	–	–	–
Along Track					
BALTR	3.99	4.01	3.99	3.99	4.00
BALTS	2.79	1.14	0.48	1.17	0.75
TBAT	6.78	5.14	4.47	5.16	4.75
RESL	72.7	85.2	70.0	91.7	88.3
RESH	–	–	–	–	–
GDRL	16.9	12.8	15.2	11.0	11.2
GDRH	–	–	–	–	–
Cross Track					
BCTR	0.72	0.82	0.71	0.72	0.77
BCTS	9.60	6.34	9.12	8.46	-0.21
TBCT	10.32	7.17	9.83	9.18	0.99
CRESL	59.2	78.4	61.5	67.7	113.1
CRESH	–	–	–	–	–
CGDRL	22.2	13.7	18.9	15.9	9.0
CGDRH	–	–	–	–	–

Table B-2 — Resolution Predictions for HPL Targets, Aft-Looking Camera, Unit No. 302

Target	119	117	125	114	124	108
Pass	37	54	56	71	71	72
Frame	13	10	112	13	50	59
X	33.9	44.4	52.3	22.6	63.3	42.4
Y	0.9	3.1	1.7	0.7	2.8	1.3
ROL	0.068	0.058	0.058	0.078	0.079	0.064
ROH	0.081	0.070	0.067	0.102	0.088	0.074
RCL	0.065	0.052	0.054	0.079	0.074	0.060
RCH	0.086	0.056	0.074	0.112	0.082	0.079
Along Track						
BALTR	3.32	3.32	3.31	3.31	3.30	3.32
BALTS	4.07	2.11	4.19	4.11	2.45	4.15
TBAT	7.39	5.43	7.50	7.42	5.76	7.46
RESL	58.7	54.5	51.8	64.7	69.9	56.0
RESH	66.2	63.8	57.6	76.2	75.5	62.0
GDRL	19.2	20.4	21.7	17.8	16.4	21.0
GDRH	17.0	17.4	19.5	15.1	15.2	18.9
Cross Track						
BCTR	0.69	0.69	0.66	0.66	0.61	0.69
BCTS	4.10	2.35	0.91	5.88	-0.96	2.77
TBCT	4.78	3.04	1.57	6.53	1.57	3.46
CRESL	61.2	51.2	53.8	67.8	73.4	58.4
CRESH	77.3	54.8	73.2	84.9	81.0	75.0
CGDRL	17.6	21.1	20.6	16.7	16.5	19.3
CGDRH	13.9	19.7	15.1	13.4	15.0	15.0

Table B-2 — Resolution Predictions for HPL Targets, Aft-Looking Camera, Unit No. 302 (Cont.)

Target	113	109	108	113	111	101
Pass	72	86	88	88	182	199
Frame	65	11	34	39	16	71
X	65.2	28.8	8.7	25.7	11.9	56.4
Y	2.5	2.0	4.5	3.7	2.9	1.8
ROL	0.068	0.074	0.047	0.065	0.094	0.068
ROH	0.081	0.086	0.052	0.071	0.111	0.078
RCL	0.063	0.068	0.046	0.054	0.087	0.062
RCH	0.076	0.092	0.050	0.066	0.129	0.086
Along Track						
BALTR	3.31	3.31	3.30	3.32	3.30	3.31
BALTS	0.42	2.19	0.19	1.65	2.60	2.28
TBAT	3.72	5.50	3.50	4.96	5.90	5.58
RESL	65.3	67.0	46.2	61.0	79.0	62.3
RESH	76.2	75.1	50.8	65.5	87.9	69.3
GDRL	19.0	16.1	25.6	17.8	13.0	16.1
GDRH	16.3	14.4	23.3	16.5	11.6	14.4
Cross Track						
BCTR	0.62	0.68	0.59	0.68	0.60	0.64
BCTS	-1.05	4.82	8.12	5.37	6.96	-0.29
TBCT	1.67	5.51	8.71	6.05	7.56	0.93
CRESL	62.6	62.4	41.8	50.6	68.9	61.9
CRESH	75.1	79.0	44.4	59.6	84.6	85.6
CGDRL	21.2	16.8	31.0	21.1	15.8	16.4
CGDRH	17.7	13.3	29.1	17.9	12.8	11.8

Table B-3 — Average Low Contrast Ground Resolution Versus Photointerpreter's Rating

The average low contrast resolution is obtained by averaging the ground resolutions for the forward- and aft-looking instruments in both along-track and cross-track directions. In other words, it is the average of four numbers.

Target Number	Average Ground Resolution, feet	Photointerpreter's Rating	Notes
119	16.7	Fair	Average of Fair ratings: 15.4 feet
117	16.5	Fair	
125	16.0	Fair	Standard deviation of Fair ratings: 1.2 feet
114	16.8	Poor	
124	14.5	Fair	Average of Poor ratings: 18.6 feet
108	16.5	Poor*	Standard deviation of Poor ratings: 3.1 feet
113	16.7	Fair	
109	14.8	Fair	
108	23.9	Poor	
113	16.3	Fair	
118	17.0	Poor	
111	13.9	Fair	
101	13.2	Fair	

NOTE: There appears to be good correlation between the photointerpreter's ratings and the predicted average ground resolution. It seems that a ground resolved distance of 16.7 feet separates the Poor from the Fair ratings. Only one target seems to contradict this conclusion. This is target no. 108 covered in pass 72 and it has been identified in Table B-3 by an asterisk. We do not know why a Poor rating was given to this target. An examination of Polaroid pictures of the original negatives indicates that there may be some thin wispy clouds over the target. Note that the photointerpreter's ratings include weather effects which have been eliminated by necessity from the predicted average ground resolution. Actually, a contradiction may not exist at all if one takes into account that the accuracy of the predicted resolution is about 0.5 foot.

Appendix C

PHOTOGRAPHIC ILLUSTRATIONS

Several photographic illustrations are included in this report to show the relative quality of the photography from this mission. The paper prints are 40× enlargements of the MIP frame and were made from the original negatives. The first photograph is from the forward camera (the MIP frame) and the second is the corresponding aft frame.

The other illustration (transparency) contains a 120× enlargement (through an A/O microscope) of the photointerpreter's duplicate positive. The split beam microscope was originally used to compare the best of this mission with the best of past missions. It then became convenient to leave both halves there for comparison purposes. The three comparisons are from past missions that had MIP ratings of 80, 85, and 90. Mission 1006 was the only one that had an MIP rating of 90. Mission 1101 has been given an MIP rating of 95. Note the detail present in the aircraft wings and engines. All of the aircraft are Boeing B-52's, although it is not possible to tell from this photograph if they are different models. The slight bulge in the sides of the fuselage of some of them indicate that there are indeed differences in models of aircraft. The absence, though, of this bulge on mission 1014 (MIP = 80) does not necessarily indicate it is not there. The engines on these aircraft have not changed very much and are, therefore, probably the best area to compare. One factor that is immediately obvious is the differences in scale of these images. The lower altitude of mission 1101 (84 nm for this image) contributed significantly to its improved quality.

Handle Via
~~Talent-KEYHOLE~~
Control System Only

[redacted]

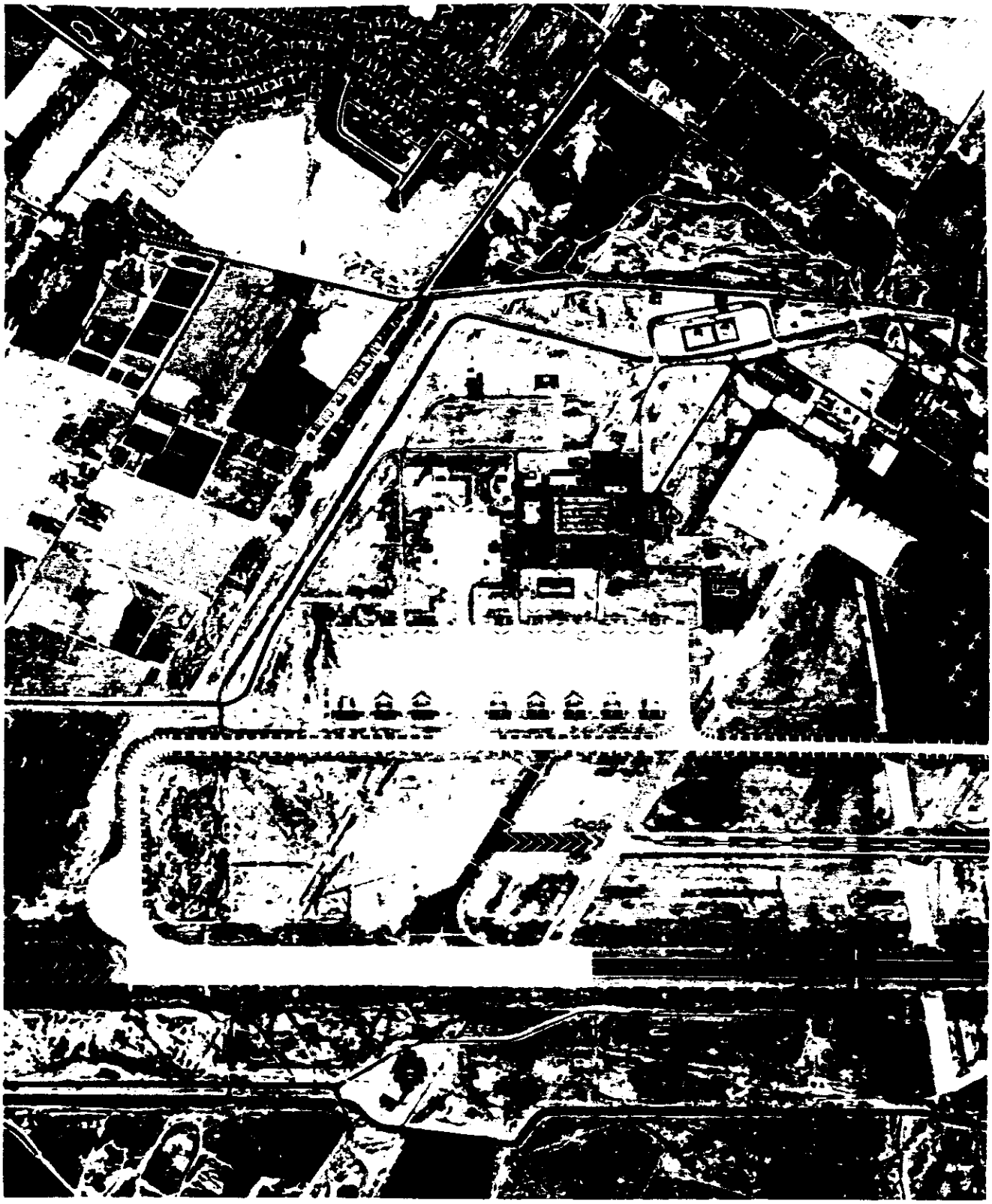

Handle Via
~~Talent KEYHOLE~~
Control System Only

[redacted]

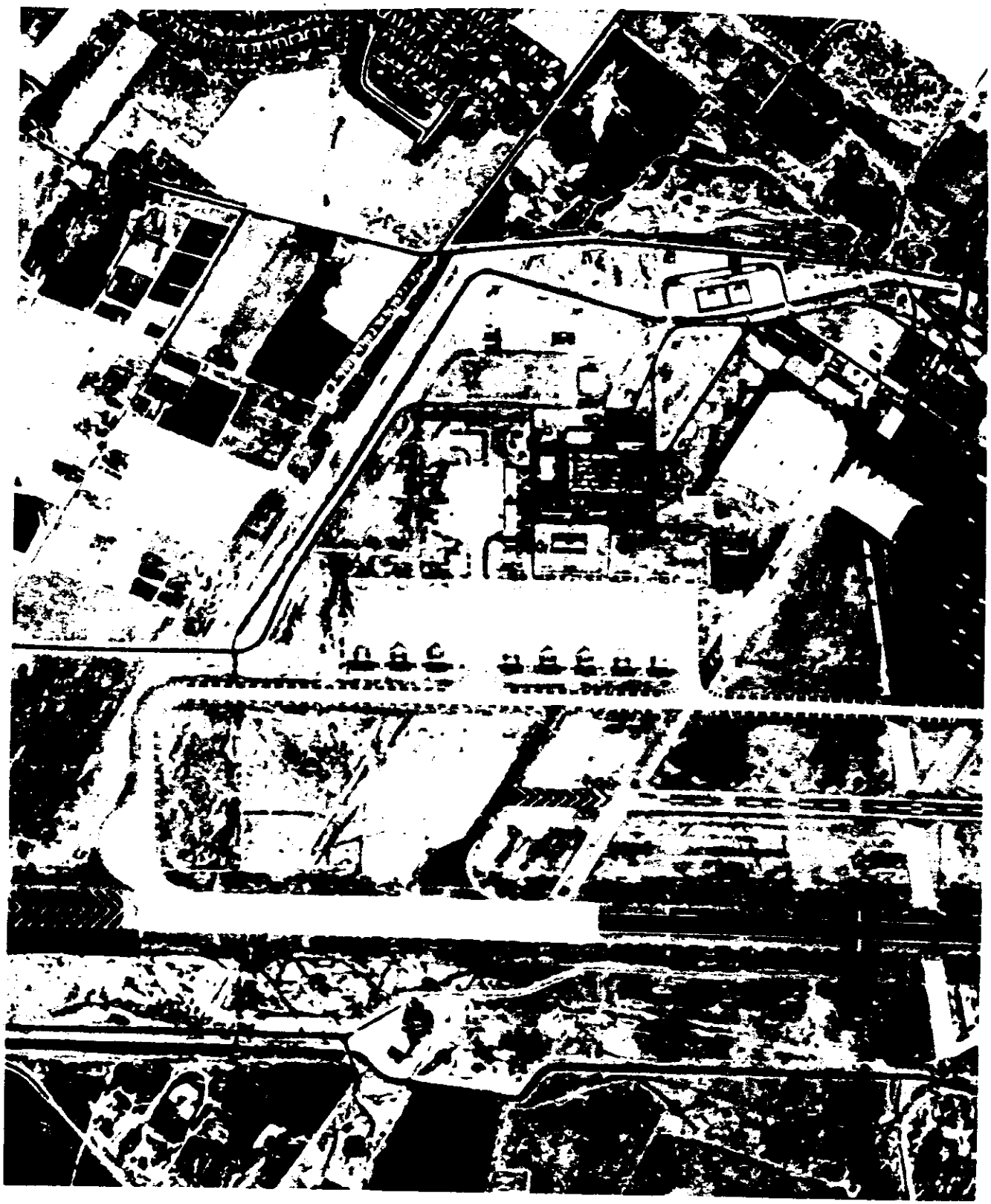

~~TOP SECRET~~

~~NO FOREIGN DISSEMINATION~~

Mission - 1006-2
Pass - D078
Camera - Aft
Frame - 019
Altitude - 105 nm
X-Coord - 52.5
System - KH-4
MIP - 90

Mission - 1025-2
Pass - D095
Camera - Aft
Frame - 015
Altitude - 113 nm
X-Coord. - 39.5
System - KH-4
MIP - 85

Mission - 1014-2
Pass - D111
Camera - Fwd
Frame - 012
Altitude - 112 nm
X-Coord. - 38.5
System - KH-4
MIP - 80

Mission - 1101-2
Pass - D159
Camera - Fwd
Frame - 002
Altitude - 84 nm
X-Coord. - 39.0
System - KH-4B
MIP - 95

120x photomicrographs of past MIP frames in comparison with that of 1101

~~TOP SECRET~~

~~NO FOREIGN DISSEMINATION~~

HANDLE VIA
~~TALENT-KEYHOLE~~
CONTROL SYSTEM ONLY

Appendix D

WEATHER ASSESSMENT

When the evaluation of the first four missions of the 1100 series is concluded, an analysis is to be performed to assess the impact of weather (principally haze) on main camera performance. The term haze has been used perhaps improperly since it is intended to include all degrading effects in the atmosphere such as water vapor, industrial pollutants, smog, dust, sand storms, and even high thin cirrus clouds (other than solid clouds) that have a degrading influence on the photography. In order to measure this degrading effect, the DISIC terrain camera is used. It gives a wide area coverage around the specific areas covered by the main panoramic cameras. It is, therefore, a good "eyeball" with which to examine the overall effects of weather. The ultimate goal of this effort is to learn about the benefits (or disadvantages) of certain haze cutting filters so far as their ability to penetrate various atmospheric conditions are concerned. This analysis will encompass all of the first four missions of the 1100 series, and will give, therefore, a sampling of an entire year of weather patterns. During this year, an effort is being carried on by HQAWS to assess the feasibility of predicting haze on a real-time basis. Their work should be concluded before 1104 and (if so), will be included in our analysis.

A significant portion of the work involves determining the haze ratio (an area weighted percentage of haze in the cloud free portions of the format). This is determined by a subjective evaluation of the DISIC imagery. An estimate is made of the amount of clear, clouds, and haze. The estimate is made of the percent of area that each of these three encompass in the format.

A tabular listing of this data will be presented in each of the first four analysis reports. The data in Tables D-1 and D-2 represent the average for all of the DISIC frames in a complete pass. However, since the DISIC can operate independently from the main camera, only those DISIC frames were used that had corresponding main camera photography.

In comparing the final averages (refer to Table D-3) with that of the preliminary mission statistics, a trend is noted. NPIC has reported somewhat more clear weather than the DISIC evaluation. However, the NPIC evaluation was performed on the main camera imagery only, and concerned itself only with the amount of clear and cloudy weather. In breaking down the clear weather portions into clear and hazy, the percent clear is greater.

Table D-1 — Weather Estimations From DISIC Photography for Mission 1101-1

Pass	Cloud, percent	Haze, percent	Clear, percent	Haze Ratio
D-005	14	38.5	47.5	45
D-006	43	–	57	–
D-008	100	–	–	–
D-009	13	08	79	9
D-014	24	33	43	43
D-016	33	13	54	19
D-021	21	12.5	66.6	16
D-022	50	16	34	32
D-024	74	12	14	46
D-025	18	07	75	8.5
D-029	44	27	29	48
D-030	31	09	60	13
D-032	40~	46	13	78
D-035	29	04	69	5.5
D-036	–	09	91	9
D-037	33	18	49	27
D-038	48	05	47	10
D-039	07.5	67.5	25	73
D-040	65	17	18	49
D-041	06	–	94	–
D-045	30	02	68	3
D-048	28	32	40	44
D-051	19	–	81	–
D-054	24	13	63	17
D-055	47	18	35	34
D-056	51	16	33	33
D-057	11	03	86	3
D-068	21	05	74	6
D-069	10	11	79	12
D-070	100	–	–	–
D-071	49	09	42	17
D-072	45	06	49	11
D-073	06	–	94	–
D-074	15	20	65	23
D-085	06	31	63	33

Mission Average

Cloud	Haze	Clear	Haze Ratio
33%	14.5%	52.5%	22

Table D-2 — Weather Estimations From DISIC Photography for Mission 1101-2

Pass	Cloud, percent	Haze, percent	Clear, percent	Haze Ratio
D-088	37	01	62	15
D-089	08	–	92	–
D-090	18	21	61	26
D-093	32	–	68	–
D-100	18	11	71	13
D-101	05	19	76	20
D-102	63	29	08	78
D-103	02	06	92	6
D-104	06	34	60	36
D-105	06	10	84	11
D-106	01	–	99	–
D-111	34	08	58	12
D-116	53	11	36	23
D-118	59	19	22	46
D-119	–	–	100	–
D-120	04	38	58	40
D-121	–	25	75	25
D-125	20	31	49	39
D-127	15	–	85	–
D-132	24	04	72	5
D-134	73	08	19	30
D-135	42	07	51	12
D-136	79	02	19	10
D-137	–	01	09	1
D-138	05	–	95	–
D-143	61	–	39	–
D-148	10	12	78	13
D-149	17	–	83	–
D-152	41	25	34	42
D-153	30	–	70	–
D-157	30	01	69	1.5
D-159	37	–	63	–
D-164	15	03	82	3
D-165	84	–	16	–
D-166	64	–	36	–
D-167	49	06	45	12
D-16801	01	15	84	15
D-170	100	–	–	–
D-172	47	28	25	53
D-173	09	35	56	38
D-175	81	–	19	–
D-179	16	–	84	–
D-181	88	–	12	–
D-182	16	–	84	–
D-183	52	–	48	–
D-184	14	–	86	–
D-190	20	–	80	–
D-195	31	–	69	–
D-196	16	18	66	21
D-198	52	–	48	–
D-199	93	05	02	71

Mission Average

Cloud	Haze	Clear	Haze Ratio
33%	8.5%	58.5%	14

Table D-3 — Weather Estimations for the Entire Panoramic Coverage Portion of the Mission

Mission	Cloud, percent	Haze, percent	Clear, percent	Haze Ratio	NPIC Evaluation, percent
1101-1	33	14.5	52.5	21.6	65
1101-2	33	8.5	58.5	12.7	70
Mission Average	33	11.5	55.5	17.1	